UNIVERSITY OF MINNESOTA
ST. ANTHONY FALLS HYDRAULIC LABORATORY

Project Report No. 335

Sediment Oxygen Demand in Lakes: Dependence on Near-Bottom Flow Velocities

by

Yoshiyuki Nakamura

and

Heinz G. Stefan

Prepared for

LEGISLATIVE COMMISSION ON MINNESOTA RESOURCES
State of Minnesota
Minneapolis, Minnesota

November 1992
Minneapolis, Minnesota

Abstract

A model of sediment oxygen demand (SOD) is presented which determines the SOD as a function of flow velocity over the sediment. A quantitative relationship is established between SOD and the velocity and dissolved oxygen concentration in the bulk water. Oxygen consumption in the sediment is expressed as the sum of biological consumption with Michaelis–Menten kinetics, and the chemical consumption assumed to be a first order reaction of oxygen. At very low flow velocities, transport through the diffusive boundary layer is the limiting factor of SOD, and SOD is expressed as a linear increasing function of velocity. On the other hand, when flow velocities are increased, SOD becomes independent of velocity, since the reactions in the sediment are the rate limiting factor. The model also suggests that SOD is an increasing function of dissolved oxygen concentration in the water overlying the sediment and that SOD has no upper limit when DO concentration is large. Combined with the linear theory of internal seiche motion an average SOD in a rectangular, two–layered lake is derived as functions of the wind velocity, aspect ratio of the lake an the depth of the thermocline. The average SOD has a minimum when the thermocline depth is 1/4 of the total depth.

Table of Contents

		Page No.
	Abstract	i
	List of Figures	iii
1.	INTRODUCTION	1
2.	MODEL FORMULATION	3
	2.1 Model concept	3
	2.2 Oxygen Transfer through the Water Boundary Layer	3
	2.3 Oxygen Uptake Processes in the Sediments	9
	2.4 Total SOD Flux	12
3.	COMPARISON OF THEORY WITH EXPERIMENTAL DATA	16
4.	ANALYSIS OF DO CONCENTRATION DEPENDENCE ON SOD IN A WATER COLUMN	19
5.	ANALYSIS OF SOD IN A RECTANGULAR, TWO-LAYERED LAKE	23
6.	CONCLUSIONS	28
	APPENDIX I – Behavior of C_w, δ_s, and C_c as a function of U_*	31
	APPENDIX II – References	35
	APPENDIX III –Notations	41

Figures 1 through 17

List of Figures

Fig. 1 Schematic distribution of dissolved oxygen concentration (a) and flow velocity (b). The boundary layer is divided into a viscous sublayer and the turbulent layer.

Fig. 2. Non–dimensional, sediment oxygen demand (SOD) as function of non–dimensional velocity and first–order reaction rate constant k_*'; (a) $K_{02*}=0$; (b) $K_{02*}=1$. (Defined in Eqs. 25 and 27)

Fig. 3. Non–dimensional, sediment oxygen demand (SOD) as function of non–dimensional velocity and half saturation constant K_{02*}: (a) $k_*'=0$; (b) $k_*'=1$.

Fig. 4. Ratio of chemical and biological reactions as function of non–dimensional velocity, K_{02*}, and k_*'.

Fig. 5. Dissolved oxygen concentration at the sediment water interface as function of non–dimensional velocity, K_{02*} and k_*': (a) $K_{02*}=0$; (b) $K_{02*}=1$; (c) $k_*'=0$; (d) $k_*'=1$.

Fig. 6. Non–dimensional thickness of the aerobic zone in the sediment as function of non–dimensional velocity and first–order reaction rate constant k_*': (a) $K_{02*}=0$; (b) $K_{02*}=1$.

Fig. 7. Non–dimensional thickness of the aerobic zone in the sediment as function of non–dimensional velocity and a half saturation constant K_{02*}: (a) $k_*'=0$; (b) $k_*'=1$.

Fig. 8. Vertical distribution of dissolved oxygen concentration as function of non–dimensional velocity: $K_{02*}=0$ and $k_*'=0$.

Fig. 9. Comparison of observed and calculated results of SOD as a function of velocity. Open circles denote measurements by Boynton et al. (1980) using an in situ chamber at three different sediments representing (a) sand, (b) sandy–mud and (c) mud environments. Estimated values of $(2D_s\mu C_\infty)^{1/2}$ and $(2f^2C_\infty/D_s\mu)^{1/2}$ are (a) 9.1 $gm^{-2}d^{-1}$ and 0.27 $cm^{-1}s$, (b) 9.0 $gm^{-2}d^{-1}$ and 0.25 $cm^{-1}s$ (7.5 and 0.35 for broken curve) and (c) 7.4 $gm^{-2}d^{-1}$ and 0.16 $cm^{-1}s$.

Fig. 10. Observed and calculated vertical distributions of dissolved oxygen concentrations. Open circles denote measurements by Joergensen and Des Marais (1990) in a laboratory experiment with a rough sediment—water interface (microbial mat) from a saline pond. The theoretical line is for a smooth wall and obtained by the theory given herein.

Fig. 11. Observed and calculated results of SOD as a function of velocity. Open circles denote measurements by Joergensen and Des Marais (1990) in a laboratory experiment with a sediment–water interface (microbial mat) from a saline pond. The theoretical lines are for a smooth wall and obtained by the theory given herein.

Fig. 12. Non–dimensional SOD as function of non–dimensional DO concentration and (a) first–order reaction rate constant k_*' and (b) half saturation constant K_{02*}.

Fig. 13. Comparison of calculated and measured SOD as function of DO concentration; data from Polak and Haffner (1978) (left) and Edwards and Rolley (1965)(right).

Fig. 14. Comparison of model predictions of DO concentration with measurements for an ice covered lake by Mathias and Barica (1980); left, a=0.1 day^{-1} right, b=0.5 m^2g^{-1}.

Fig. 15. Non–dimensional, space and time averaged SOD in a rectangular, two–layered lake as function of non–dimensional maximum velocity due to internal standing wave. Dotted line represents an asymptotic solution at low velocity. Broken curve denotes a proposed approximate function of averaged SOD.

Fig. 16. SOD averaged over time and bottom area in a two–layered lake versus non–dimensional parameter including wind shear and fetch. h_* is the relative depth of the hypolimnion.

Fig. 17. SOD averaged over time and bottom area in a two–layered lake versus non–dimensional depth of the hypolimnion. τ_* is the windshear parameter.

1. INTRODUCTION

Dissolved oxygen depletion in lakes and estuaries has been a serious problem, as it damages fisheries and ecosystems. Sediment oxygen demand (hereafter referred to as SOD) and water column respiration both contribute to oxygen depletion in the lower layers of natural water bodies such as rivers, lakes, reservoirs, ponds and embayments. SOD is a dominant sink of dissolved oxygen in certain rivers (Hanes and Irvine, 1968), in lakes (Burns, 1970; Mathias and Barica, 1980), and in estuaries (Officer et al., 1984). SOD depends on water depth (Mathias and Barica, 1980; Ellis and Stefan, 1989) and the trophic state (Hargrave, 1973; Mathias and Barica, 1980; Belanger, 1981).

Belanger (1981) and Boynton et al. (1981) showed a significant effect of flow velocity on SOD using a flow-through system in a laboratory and a closed chamber in situ, respectively. SOD was shown to change by an order of magnitude as flow velocities of the water overlying the sediments were changed. The effect of velocity on DO transfer is attributed to the following two reasons; (1) increasing diffusion coefficient in the boundary layer and (2) decreasing boundary layer thickness and hence increasing the DO gradient when flow velocities increase. Velocity effects also manifest themselves indirectly when lake aeration system designed for SOD values measured in quiescent water are unable to maintain the expected DO levels when the water is agitated. The flow velocities induced near the sediment by these devices are considered to be the reason for the increased oxygen demand (Stefan, 1990).

Following the results of Belanger (1981) and others, many researchers have made experiments using stirring devices (Berelson and Hammond, 1990; Jahnke, 1990; Hickes, 1990; Whittemore, 1990). However, no theoretical work on the velocity effect appears to have been performed. The purpose of this study, therefore, is to present an analysis of the effect of flow velocity on SOD in aquatic environments.

2. MODEL FORMULATION

2.1 MODEL CONCEPT

Dissolved oxygen (DO) must traverse two diffusive boundary layers to travel from the water column into the sediment where it is consumed by bacteria and by chemical reactions: one is in the water immediately above the sediments and the other in the sediments immediately below (Fig. 1). It is justified to assume that there is no consumption of DO in the water boundary layer. The following analysis will examine first each of these two boundary layers separately and then combine them to calculate the total flux of DO from the water to the sediments (SOD). The boundary layers will be treated as fully developed because of the typically large horizontal dimensions of lakes relative to the boundary layer thickness.

2.2 OXYGEN TRANSFER THROUGH THE WATER BOUNDARY LAYER

In order to model the oxygen transfer in the fully developed boundary layer near the sediment/water interface, the following assumptions will be made:

1. steady state
2. sediment surface is a fixed, smooth flat bed,
3. velocity and DO concentration are homogeneous except in vertical direction,
4. the boundary layer is thin enough to ignore DO consumption in it and to approximate the shear stress to be constant.

With these assumptions, it is possible to apply the analyses of turbulent heat transfer made by Prandtl (1910), von Karman (1939) and Deissler (1951) to mass (dissolved oxygen) transfer near the wall.

Following the theory by Prandtl (1910) on heat transfer in the turbulent boundary layer, the boundary layer is divided into a viscous (laminar) sublayer and a turbulent region as shown in Figure 1.

Momentum equation and conservation of DO are written as follows.

$$\frac{\tau}{\rho} = (\nu+K_M)\frac{du}{dy} \tag{1}$$

$$J = -(D+K_y)\frac{dC}{dy} \tag{2}$$

where τ, ρ, ν, K_M, J, D, K_y, u, C and y are shear stress, density, kinematic viscosity, turbulent diffusivity for momentum vertical flux of DO, molecular diffusivity of DO, turbulent diffusivity for DO, velocity, DO concentration, and the vertical coordinate from the sediment-water interface (positive upward). The boundary conditions are

$$u = 0,\ C = C_w \quad \text{at } y = 0 \tag{3a}$$

$$u = u_\ell,\ C = C_\ell \quad \text{at } y = \delta_\ell \tag{3b}$$

$$u = u_\infty,\ C = C_\infty \quad \text{at } y = \infty \tag{3c}$$

where δ_ℓ is the thickness of the viscous sublayer.

If we define the Schmidt number and the turbulent Schmidt number, respectively, as

$$S_c = \nu/D, \quad S_{ct} = K_M/K_y \tag{4}$$

then the DO flux is rewritten as follows

$$J = -\left(\frac{\nu}{S_c} + \frac{K_M}{S_{ct}}\right)\frac{dC}{dy} \tag{5}$$

In the turbulent layer, the turbulent diffusivities K_M, K_y are larger than ν and D respectively. On the other hand, in the viscous sublayer, the turbulent diffusivities can be ignored. Therefore,

$$\frac{J}{\tau/\rho} = -\frac{D}{\nu}\frac{dC}{du} : \quad \text{viscous sublayer} \tag{6a}$$

$$\frac{J}{\tau/\rho} = -\frac{K_y}{K_M}\frac{dC}{du} : \quad \text{turbulent layer} \tag{6b}$$

τ and J are constant with depth, hence $J/(\tau/\rho)$ is constant with depth.

Integrating (6) within the two layers, and considering the boundary conditions (3) gives

$$\frac{J}{\tau/\rho} = -\frac{D}{\nu}\frac{C_\ell - C_w}{u_\ell} : \text{viscous sublayer} \tag{7a}$$

$$\frac{J}{\tau/\rho} = -\frac{K_y}{K_M}\frac{C_\infty - C_\ell}{u_\infty - u_\ell} : \text{turbulent layer} \tag{7b}$$

Since the flux ratio, $J/(\tau/\rho)$, is identical within the two layers,

$$\frac{1}{S_c}\frac{C_\ell - C_w}{u_\ell} = \frac{1}{S_{ct}}\frac{C_\infty - C_\ell}{u_\infty - u_\ell} \tag{8}$$

or

$$S_c(C_\infty - C_w) = \{S_c + S_{ct}(u_\infty/u_\ell - 1)\}(C_\ell - C_w) \tag{9}$$

Substituting (9) into the first equation of (7) and with $S_{ct}=1.0$, the DO flux is expressed as

$$J = -\frac{C_f}{2}\frac{u_\infty}{1+\frac{u_\ell}{u_\infty}(S_c-1)}(C_\infty - C_w) \tag{10}$$

where C_f is the friction coefficient defined by

$$C_f = \frac{\tau}{\frac{1}{2}\rho u_\infty^{\,2}} \tag{11}$$

Equation (10) was derived by Prandtl (1910) and Taylor(1916) for heat transfer.

In order to apply eq. (10) to a real situations, u_ℓ/u_∞ must be evaluated. According to von Karman (1939), the thickness of the laminar sublayer δ_ℓ is given as

$$\frac{u_* \delta_\ell}{\nu} = 5 = \frac{u_\ell}{u_*} \tag{12}$$

where $u_*(=\sqrt{\tau/\rho})$ is the shear velocity. Therefore,

$$\frac{u_\ell}{u_\infty} = 5\sqrt{\frac{1}{2}C_f} \tag{13}$$

If (13) is used to eliminate u_ℓ, then the DO flux can be written as follows:

$$J = -\frac{\frac{1}{2}C_f}{1+5\sqrt{\frac{1}{2}C_f}(S_c-1)} u_\infty(C_\infty-C_W) \tag{14}$$

Von Karman (1939) subdivided the velocity profile into three layers; a turbulent region, a buffer layer and a viscous sublayer. He assumed that the flow in the laminar sublayer is completely laminar, so that the term with the turbulent diffusivities vanishes in Eqs. (1) and (2). In addition, he assumed that the turbulent Schmidt number is unity both in a buffer layer and a turbulent region. The following equation was then derived for the mass flux.

$$J = -\frac{\frac{1}{2}C_f}{1+5\sqrt{\frac{1}{2}C_f}\{(S_c-1)+\ln\frac{1+5Sc}{6}\}} u_\infty(C_\infty-C_W) \tag{15}$$

The above equation gives an accurate estimation of J for a flat plate as well as for a tube when the Schmidt number is smaller than 5 (Shirozuka et al., 1966; Katto, 1964). If we assume $S_{ct}=1$ we can modify Eq. (5) to

$$\frac{dC}{dy} = - \frac{J/\nu}{(1/S_c)+(K_M/\nu)} \qquad (16)$$

In order to estimate flux of solutes with Sc=500, which is a typical value for oxygen in pure water, K_M/ν must be evaluated precisely down to 1/500 or less. This parameter cannot be neglected even in the viscous sublayer, since intermittent turbulence exists in the layer. This is the reason why von Karman's equation is not valid for larger Sc.

Von Karman's approach was modified by several investigators, most successfully by Deissler (1951, 1954), who used the following two relationships:

$$K_M/\nu = n^2 u^+ y^+ \{1-\exp(-n^2 u^+ y^+)\} \qquad \text{when } y^+ \leq 26 \qquad (17a)$$

$$K_M/\nu = k^2 \frac{(du^+/dy^+)^3}{(d^2u^+/dy^{+2})^2} \qquad \text{when } y^+ > 26 \qquad (17b)$$

where u^+ and y^+ are non-dimensional velocity and vertical coordinates defined by

$$u^+ = u/u*, \quad y^+ = yu*/\nu \qquad (18)$$

and n (=0.109) and k (=0.36) are numerical constants. For mass or heat transfer with large Sc (Pr) number, Eq. (17a), which is valid near the wall, is more important. Expanding the equation as a Taylor series around $y^+=0$ and assuming that $u^+=y^+$, we obtain

$$K_M/\nu = (ny^+)^4 \qquad (19)$$

Substituting (19) into (16) gives

$$\int_{C_W}^{C_\infty} dC = -\int_0^\infty \frac{J/\nu}{(1/S_c)+(nu_*/\nu)^4 y^4}\, dy \qquad (20)$$

With some algebra, the mass flux is expressed as

$$J = -f(C_f, S_c)u_\infty(C_\infty - C_W) = -\frac{2}{\pi} n \sqrt{C_f} S_c^{-3/4} u_\infty (C_\infty - C_W) \qquad (21)$$

Some investigators have proposed a different power law in Eq. (19) and a different Sc number dependence in Eq. (21) based on theoretical considerations (e.g. Monin and Yaglom, 1965). Shaw and Hanratty (1977) showed experimentally that J is proportional to $S_c^{-0.704}$ for large Schmidt numbers, which is close to Eq. (21). Eq. (21) predicts heat and mass transfer rates in good agreement with experimental results up to $S_c \approx 4000$ (Katto, 1964).

Mass flux is often expressed in terms of a mass transfer coefficient, k_A, or a thickness of the diffusive boundary layer, δ_c. Definitions of these parameters are shown in Appendix I.

2.3 OXYGEN UPTAKE PROCESSES IN THE SEDIMENTS

Walker and Snodgrass (1986) expressed SOD as follows:

$$SOD = \mu_\beta \frac{C_\infty}{Ko_2 + C_\infty} + k_c C_\infty \qquad (22)$$

where μ_β and k_c are rate constants and Ko_2 is a half saturation constant. The first term in Eq. (22) represents "Biological SOD" and the second "Chemical SOD", respectively.

They formulated Eq. (22), assuming that the oxidation of organic matter in the aerobic zone is the rate controlling step for B-SOD and that oxygen consumption by C-SOD is mass transfer limited. Then, total volumetric oxygen consumption in the sediments, R, was expressed as

$$R = \mu \frac{C_\infty}{Ko_2 + C_\infty} + \frac{1}{\delta_s} D_s \frac{dC}{dy} \Big|_{y=0} \qquad (23)$$

where μ is the maximum aerobic oxidation rate, δ_s is the depth of the aerobic zone and D_s is the apparent diffusivity of oxygen in the sediment. Assuming $dC/dy \simeq C_\infty/\delta_s$, they integrate R with depth to obtain SOD as (22), where

$$\mu_\beta = \mu\delta_s, \quad k_c = D_s/\delta_s \qquad (24)$$

Eq.(22) is a simple expression of SOD, which has only three coefficients Ko_2, μ_β and k_c. However μ_β and k_c are dependent on δ_s. Since δ_s, depth of aerobic zone, is affected by biological activities and velocity of the overlying water, μ_β and k_c are also affected by them. If SOD is dependent on velocity, μ_β and k_c are not appropriate independent parameters for SOD.

Therefore, we will consider a slightly different formulation. If we assume that the chemical reaction is a first order reaction of DO concentration, then

$$R = \mu \frac{C_w}{Ko_2 + C_w} + k'C_w \qquad (25)$$

where bulk DO concentration C_∞ is replaced by DO concentration at the interface, C_w, in Eq. (25) and k' is the first order rate constant. If we put $k'=D_s/\delta_s^2$, Eq.(25) coincides with Eq. (22). (Assume $dC/dy \approx C_w/\delta_s$.) More rigorously, C_w should be replaced by a local concentration of DO. But as a first approximation, we adopt Eq. (25).

Bouldin (1968) solved the diffusion equation for dissolved oxygen concentration in the sediment, assuming D_s and R are constant with depth, and obtained

$$SOD = \sqrt{2D_s R C_w} \qquad (26)$$

The advantage of Eq. (25) is that R is constant so that Bouldin's analysis is easily extended to

$$SOD = \sqrt{2D_s C_w \left(\mu \frac{C_w}{Ko_2 + C_w} + k'C_w\right)} \qquad (27)$$

From Eqs. (21) and (27), we can eliminate C_w. Considering that -J should be identical to SOD, we arrive at the following formula.

$$\left(\frac{k'}{f^3 u_\infty^3} - \frac{1}{2D_s f u_\infty}\right) SOD^3 - \left\{\frac{k'(3C_\infty + Ko_2) + \mu}{f^2 u_\infty^2} - \frac{Ko_2 + C_\infty}{2D_s}\right\} SOD^2$$

$$+ \frac{k'(3C_\infty + 2Ko_2) + 2\mu}{u_\infty} C_\infty SOD - \{k'(C_\infty + Ko_2) + \mu\} C_\infty^2 = 0 \qquad (28)$$

Non-dimensional parameters are introduced as follows:

$$SOD_* = \frac{SOD}{\sqrt{2D_S \mu C_\infty}}, \quad U_* = fu_\infty \sqrt{\frac{2C_\infty}{D_S \mu}}, \quad Ko_{2*} = \frac{Ko_2}{C_\infty}, \quad k'_* = \frac{k'C_\infty}{\mu} \qquad (29)$$

Using Eq. (29), Eq. (28) can be rewritten in non-dimensional form as:

$$2\left(4\frac{k'_*}{U_*^3} - \frac{1}{U_*}\right)SOD_*^3 - \left\{\frac{4\{k'_*(3+Ko_{2*})+1}{U_*^2} - (Ko_{2*}+1)\right\}SOD_*^2$$

$$+ \frac{2\{k'(3+2Ko_{2*})+2\}}{U_*}SOD_* - \{k'_*(1+Ko_{2*})+1\} = 0 \qquad (30)$$

2.4 TOTAL SOD FLUX

To obtain SOD_*, Eq. (30) must be solved. The solution for SOD_* can be analysed separately for the following conditions: When $k'_*=0$ and $Ko_{2*}=0$, Eq. (30) reduces to

$$-\frac{2}{U_*}SOD_*^3 - \left(\frac{4}{U_*^2}-1\right)SOD_*^2 + \frac{4}{U_*}SOD_* - 1 = 0 \qquad (31)$$

and the solution is

$$SOD_* = \frac{-1+\sqrt{1+U_*^2}}{U_*} \qquad (32)$$

or when $Ko_{2*}=0$ Eq. (30) reduces to

$$SOD_* = \frac{(k'_*+1)U_*}{2k'_*+1+\sqrt{(k'_*+1)U_*^2+1}} \qquad (33)$$

As will be explained later, $Ko_{2*}=0$ is a good approximation except for anoxic or highly oxygen-depleted waters, since Zobell (1943) showed Ko_2 to be about 0.5 gm^{-3}. Therefore, Eq. (33) gives an approximate solution when dissolved oxygen concentration is not low.

Some interesting cases are worth consideration. For example, in the limit $k'_* \to \infty$,

$$\lim_{k'_* \to \infty} SOD_* = \frac{1}{2} U_* \qquad (34)$$

Eq. (34) means that the chemical reaction is so fast that the diffusion in the boundary layer is the limiting process.

Another example is the case of $U_* \to 0$. In this case,

$$\lim_{U_* \to 0} SOD_* = \frac{1}{2} U_* \qquad (35)$$

This also shows that the diffusion in the boundary layer is the controlling process.

One more limiting case is $U_* \to \infty$. In this case, the boundary layer thickness is so small that the diffusion process cannot be the rate controlling factor any more. SOD_* is, therefore, determined by Ko_{2*} and k'_*.

$$\lim_{U_* \to \infty} SOD_* = \sqrt{k'_* + \frac{1}{1+Ko_{2*}}} \qquad (36)$$

The basic equation (30) is solved numerically by the Newton method. Calculated results are shown in Figs. 2 and 3.

In Fig. 2(a), Ko_{2*} is fixed to be zero and k'_* is varying from zero to infinity. $Ko_{2*}=0$ means that the biological reaction is a 0-order reaction (see Eq. (25)). $k'_*=0$ means that there exists no chemical reaction. With increasing k'_*, SOD_* becomes larger. In the limit of $k'_* \to \infty$, SOD_* approaches $(1/2)U_*$ as already discussed above.

In Fig. 2(b), Ko_{2*} is fixed to be unity, which means that the bulk DO concentration is as small as the half saturation constant. Compared with Fig. 2(a), SOD_* has smaller values. In the limit of large flow velocity ($U_* \to \infty$), SOD_* approaches $(k'_*+0.5)^{1/2}$ (see Eq. (36)) in this figure, while it approaches $(k'_*+1)^{1/2}$ in Fig. 2(a).

Fig. 3 shows results with fixed k'_*. Fig. 3(a) applies when there is no chemical reaction and Fig. 3(b) shows the results when chemical reaction takes place at the same order of magnitude as the biological reaction, since $k'_*=1$ means $k'C_\infty=\mu$ (see Eq. (29)). With increasing Ko_{2*}, SOD_* becomes smaller, since the biological reaction decreases from its maximum value of μ. In the limit of $Ko_{2*} \to \infty$, the biological reaction does not take place any more. Therefore, the results for $Ko_{2*} \to \infty$ show "pure" chemical reaction.

A comparison of magnitude of the chemical and biological reactions is informative. The ratio r is introduced as follows:

$$r = \frac{\text{chemical reaction rate}}{\text{biological reaction rate}} = \frac{k'C_W}{\mu C_W/(Ko_2+C_W)}$$

$$= k'_*(Ko_{2*}+1-2\frac{SOD_*}{U_*}) \tag{37}$$

In the limit $U_* \to \infty$, SOD_*/U_* approach zero. Therefore,

$$\lim_{U_* \to \infty} r = k'_*(Ko_{2*}+1) \tag{38}$$

On the other hand, in the limit $U_* \to o$,

$$\lim_{U_* \to 0} r = k'_* Ko_{2*} = k'Ko_2/\mu \tag{39}$$

because SOD_* approaches $(1/2)U_*$ in the limit. Eq. (39) shows that the chemical reaction makes a smaller contribution when flow velocity is low. Especially for $Ko_{2*}=0$, there exists no chemical reaction. Fig. 4 shows r vs. U_* as a function of Ko_{2*} and k'_*.

The behavior of the DO concentration C_W at the sediment-water interface and the depth of the aerobic zone δ_s is shown in Figs. 5, 6 and 7 (see Appendix I for details).

3. COMPARISON OF THEORY WITH EXPERIMENTAL DATA

Theoretical predictions of SOD vs. flow velocity are compared with experimental results by Boynton et al. (1980) in Fig. 9. They made experiments using in situ chambers fitted with variable speed pumps and found a strong, positive relationship between flow velocity and SOD. During the experiments, DO concentration never fell below 3.0 ppm, which is much smaller than a typical value of Ko_2 (e.g. Zobell, 1943; Zobell and Brown, 1944). They concluded that C-SOD was small compared with B-SOD at three sites in the Patuxent River Estuary. Therefore, $Ko_{2*}=0$ and $k'_*=0$ were used in Fig. 9. Since observed values of $R(\mu)$, f and C_∞ are not available, calculations in Fig. 9 shows curve-fitted results. However, calculated results well reproduced the increase of SOD with flow velocity. During experiments using sandy mud as sediments, they observed increased SS concentration due to sediment resuspension at a velocity of 20 cm/s. Therefore, we calculated two fitted curves including and excluding the value at 20 cm/s.

This model can predict the DO distribution in and above the sediment. Fig.8 is a typical example of calculated results with varying U_*, in which $Ko_{2*}=0$, $k'_*=0$ and $D_S/D=0.5$. Recent development of microelectrodes has enabled precise measurements of vertical distribution of DO concentrations near the water-sediment interface. Joergensen and Revsbech (1985) observed that the thickness of the diffusive boundary layer over the sediment depended on the flow velocity; at higher velocity, the

thickness was smaller. DO concentration at the interface and the thickness of the aerobic zone in the sediments are increased at higher velocities (Joergensen and Revsbech, 1985; Gundersen and Joergensen, 1990). These observed facts are well reproduced in our calculations, which suggests reliability of our model.

The theory and the experimental data presented so far are for a hydrodynamically smooth boundary (wall) which is considered a realistic and meaningful condition for freshwater lake beds consisting of organic materials. Hydrodynamically rough sediment-water interfaces are, however, not unrealistic as shown by Joergensen and Des Marais (1990) for saline ponds. Their investigation provided the detailed topographic microstructure of the sedimentary surface as well as the dissolved oxygen profiles in the diffusive boundary layer (less than 1 mm thick) immediately above the sediment surface. In their experiments roughness increased sedimentary oxygen demand because of an increase of effective surface area of the sediment-water interface and by reduction of the diffusive boundary layer thickness relative to a flat plane.

Joergensen and Des Marais' (1990) experimental data cannot be described by the theory for a smooth flat wall presented herein. There is some agreement between calculated and observed boundary layer thickness (Fig. 10), but the SOD fluxes measured on a rough boundary are, not surprisingly, larger than those predicted by the smooth wall theory, especially at low velocities (Fig. 11). A theory for a rough boundary layer is needed to explain mass and heat transfer rates up to three and

four times compared to smooth surfaces (Dawson and Trass, 1972; Eckert and Drake, 1972). We believe that roughness of 4 mm height as used by Joergensen and Des Marais (1990) are not typical of freshwater lake bottoms, but further investigations, especially in situ, are necessary to prove or disprove this claim.

4. ANALYSIS OF DO CONCENTRATION DEPENDENCE ON SOD IN A WATER COLUMN

In order to compare the SOD formula with field experiments or DO observations in lakes, bays or even rivers, the new formula desired herein is rewritten as an explicit function of the bulk DO concentration, C_∞. Non-dimensional parameters have been defined previously in Eq.(29), with DO concentration as an independent parameter. Now the velocity is assumed to be an independent parameter and new non-dimensional parameters are defined as follows:

$$\hat{SOD} = \frac{fu_\infty}{D_s \mu} SOD, \quad \hat{C}_\infty = \frac{2f^2 u_\infty^2}{D_s \mu} C_\infty, \quad \hat{K}_{O_2} = \frac{2f^2 u_\infty^2}{D_s \mu} K_{O_2},$$

$$\hat{k}' = \frac{D_s}{2f^2 u_\infty^2} k' \tag{40}$$

The basic equation (28) is then rewritten as:

$$(2\hat{k}' - \frac{1}{2})\hat{SOD}^3 - \{\hat{k}'(3\hat{C}_\infty + \hat{K}_{O_2}) + 1 - \frac{1}{4}(K_{O_2} + \hat{C}_\infty)\}\hat{SOD}^2$$

$$+\{\hat{k}'(\frac{3}{2}\hat{C}_\infty + \hat{K}_{O_2}) + 1\}\hat{C}_\infty \hat{SOD} - \frac{\hat{C}_\infty^2}{4}\{\hat{k}'(\hat{C}_\infty + \hat{K}_{O_2}) + 1\} = 0 \tag{41}$$

The above equation has a simple solution when $\hat{k}'=0$ and $\hat{Ko}_2=0$, which is equivalent to the condition that the oxygen consumption is a zero-order reaction, as follows:

$$\hat{SOD} = -1 + \sqrt{1+\hat{C}_\infty} \qquad (42)$$

A significant feature of the solution is that there is no upper limit of SOD when the DO concentration becomes large. This also holds true when $\hat{k}' \not\ll 0$ or $\hat{Ko}_2 \not\ll 0$. At low DO concentrations, SOD is a linearly increasing function of DO. Solutions of Eq.(41) are plotted in Fig. 12 with different values of $\hat{Ko}_2$ and $\hat{k}'$. Experimental results using river mud (Edwards and Rolley, 1965) and lake sediment (Davis and Herdendorf, 1986) are plotted in Fig. 13. The increase of SOD with DO concentration is indicated by the data and reproduced by the model. A rigorous quantitative comparison between observed and theoretical values cannot be made, since no specific values of parameters (f, u, Ds, Ko_2, μ and k') are cited in the literature.

Another application is winter oxygen depletion in ice covered lakes. Mathias and Barica (1980) observed that DO concentration integrated over the whole water column decreased almost linearly in the first phase of the ice-cover period, and that DO depletion rates diminished gradually when the DO concentration fell to low levels. Consider the DO budget of the ice covered lake, assuming, for simplicity, that water column respiration is negligible compared with SOD and that parameters other than DO concentration are constant. The DO budget of the lake is expressed as

$$\frac{dC_\infty}{dt} = -\frac{1}{H} SOD \qquad (43)$$

with the initial condition

$$C_\infty = C_\infty(0) \text{ at } t=0 \tag{44}$$

where H is the total depth of a lake. Coupled with Eq. (42), the solution for DO concentration is

$$t = \frac{1}{a}\{2(A-B) + \ln\frac{A-1}{A+1} - \ln\frac{B-1}{B+1} + \ln\frac{HC\infty(0)}{HC\infty(t)}\} \tag{45}$$

where

$$A = \sqrt{1+bHC_\infty(0)},\ B = \sqrt{1+bHC_\infty(t)},$$

$$a = 2fu_\infty/H, \qquad b = 2f^2u_\infty^2/D_s\mu H \tag{46}$$

Calculated results are shown in Fig. 14, together with data. A best fit was obtained when $a=0.1\ day^{-1}$ and $b=0.5\ m^2g^{-1}$. With $D=1.3\times10^{-5}\ cm^2s^{-1}$ and H=3.1 m, $a=0.1\ day^{-1}$ is equivalent to the diffusive boundary layer thickness $\delta_c=0.7$ mm (see Eq. (A15) in Appendix II) and $b=0.5\ m^2g^{-1}$ is equivalent to $D_s\mu=0.034\ gm^{-1}d^{-2}$. The model as well as the data show that DO depletion rate decreases as DO concentration becomes small. The reduced rate at low DO concentration is explained by a smaller concentration gradient of DO in the boundary layer, even if Michaelis-Menten kinetics of DO consumption is not considered.

A similar analysis was made by Hall et al. (1989) to explain depletion rate of DO concentration in a submerged

chamber, which was designed for SOD measurement. They also assumed a constant consumption rate R, which leads to zero-order reaction, and the boundary layer resistance. Their calculated results were in good agreement with observed data. Estimated δ_c and $D_s\mu$ values were 0.8-1.7 mm and 0.0074-0.153 $gm^{-1} d^{-2}$, respectively, which are comparable with values estimated in our analysis.

5. ANALYSIS OF SOD IN A RECTANGULAR, TWO-LAYERED LAKE

Consider the SOD in lakes. Lake SOD is related to the trophic state of a lake, its depth and especially the composition of the lake bed. Thomann et al. (1987) report values of SOD from 0.2 to 1.0 $gm^{-2}d^{-1}$ for sandy lake bottom. A wide range of values up to 10 $gm^{-2}d^{-1}$ have been reported in shallow eutrophic lakes. Water motion is necessary to activate the high SOD as shown by the following analysis. The proposed formula of SOD requires information on the velocity, which is difficult to obtain in lakes. For this analysis, an internal standing wave (seiche motion) induced by wind in a rectangular, two-layered lake will be considered. For simplicity, the basic mode of oscillation with one nodal line is considered.

The linear theory of two-layered fluid motion shows that the velocity in the lower layer can be expressed as (Turner, 1973):

$$u_2 = \frac{1}{2}\left(\frac{h_1+h_2}{\varepsilon g h_1 h_2}\right)^{1/2} \frac{\tau_w}{\rho_2} \frac{\ell}{h_2} \sin\kappa x \sin\sigma t \qquad (47)$$

where $\varepsilon = (\rho_2 - \rho_1)/\rho_1$, h_1 and h_2 are depth of the upper and lower layers, τ_w is the shear stress applied at the water surface, ℓ is the fetch, κ is the wave number and σ is the angular frequency. In case of iso-thermal (non-stratified) condition, the velocity is expressed as:

$$u_2 = \frac{1}{2} \frac{1}{\sqrt{gH}} \frac{\tau_w}{\rho} \frac{\ell}{H} \sin\kappa x \sin\sigma t \qquad (48)$$

where H is the total depth. A space and time averaged SOD during a seiche motion is

$$\bar{\bar{SOD}} = \frac{1}{T}\int_0^T \frac{1}{\ell}\int_0^{\ell} SOD \; dx \; dt \qquad (49)$$

where $T(=2\pi/\sigma)$ is the period of the internal seiche.

The time scale of oxygen transfer through the boundary layer is given as δ^2/D. Joergensen and Revsbech (1985) showed that this time scale is 1.2 - 9 min, which is much shorter than a typical value of T. Therefore, we can expect that Eq. (30), which is derived for steady state, holds true at any moment of the seiche motion.

For simplicity, we put $Ko_{2*}=0$ and $k'_*=0$ so that we can use Eq.(32). Zobell (1943) and Zobell and Brown (1944) found that $Ko_2 \approx$ 0.5 mg/ℓ. Their results suggest that the bacterial consumption of DO is expected to be a zero-order reaction over a wide range of DO concentrations, although some researchers reported more higher values of Ko_2(e.g. Walker and Snodgrass, 1986). Practical, traditional DO models for lakes, streams and embayments often include the SOD contribution by a zero order process.

Belanger (1981), and Walker and Snodgrass (1986) showed that the amount of DO removed by the chemical reaction in the sediment is small compared with the biological one. In that case it is justified to put k' to be zero so that we can use Eq.(32) as a good approximation. For sediments with larger

contribution by chemical reaction (see Joergensen and Fenchel, 1974; Dale, 1978), Eq. (33) should be used instead of (32).

The averaged, non-dimensional SOD over the fetch and the period is expressed as follows:

$$\bar{\bar{SOD}}^* = \bar{\bar{SOD}}/\sqrt{2D_s \mu C_\infty}$$

$$= \left(\frac{2}{\pi}\right)^2 \left[\int_0^{\pi/2} \mathrm{Arctan}(pu_{max}\sin\theta)\,d\theta - \int_0^{\pi/2} \frac{\ln(1+p^2 u_{max}^2 \sin^2\theta)}{2pu_{max}\sin\theta}\,d\theta \right] \quad (50)$$

where:

$$u_{max} = \begin{cases} \frac{1}{2}\left(\frac{h_1+h_2}{\varepsilon g h_1 h_2}\right)^{1/2} \frac{\tau_w}{\rho_1} \frac{\ell}{h_2} & : \text{two-layered} \\ \frac{1}{2} \frac{1}{\sqrt{gH}} \frac{\tau_w}{\rho} \frac{\ell}{H} & : \text{homogeneous} \end{cases} \quad (51)$$

and

$$p = (2f^2 C_\infty / D_s \mu)^{1/2} \quad (52)$$

Calculated results of Eq.(50) are shown in Fig. 15. The averaged, non-dimensional SOD approaches unity when $pu_{max} \to \infty$. On the other hand, $\bar{\bar{SOD}}_* \to (2/\pi^2) pu_{max}$ when $pu_{max} \to 0$. Considering these features, we can approximate the average SOD_* by the following simple function:

$$\bar{SOD}_* = \frac{pu_{max}}{\pi^2/2 + pu_{max}} \tag{53}$$

In Fig. 15, the comparison is made between Eq. (53) and the exact integration of Eq. (50). The relative error is less than 10 % with pu_{max} less than 10.

Eq. (53) can be rewritten as follows when the system is stratified:

$$\bar{SOD}_* = \frac{p}{2}\frac{\tau_w/\rho_1}{\sqrt{\varepsilon g\bar{H}}}\frac{\ell}{\bar{H}} \Big/ \left\{ \left(\frac{\pi^2}{2}\right)\sqrt{h_*^3(1-h_*)} + \frac{p}{2}\frac{\tau_w/\rho_1}{\sqrt{\varepsilon g\bar{H}}}\frac{\ell}{\bar{H}} \right\} \tag{54}$$

where h_* is the relative depth of h_2 defined by

$$h_* = h_2/H \tag{55}$$

The above equation shows that the time and area averaged SOD in a lake is an increasing function of wind velocity expressed through the windshear , τ_w, the aspect ratio of the lake and the parameter p. By simple algebra, the averaged SOD is shown to have a minimum value when h_*=3/4. In Figs. 16 and 17, the averaged SOD is plotted against $\tau_* = \frac{p}{2}\frac{\tau_w/\rho_1}{\sqrt{\varepsilon g\bar{H}}}\frac{\ell}{\bar{H}}$ and h_*, respectively, with the remaining parameter in each figure. Since velocity is largely dependent on the position of the thermocline, the averaged SOD is sensitive to h_*.

Eqs. (53) and (54) are useful formulae to predict SOD and hence oxygen budgets in stratified lakes. These equations clearly show that SOD in lakes is not a constant but strongly

dependent on water motion induced e.g. by wind. These are directly applicable to most comprehensive ecological models of lake water quality (e.g. MINLAKE by Riley and Stefan, 1988).

6. CONCLUSIONS

A model for sediment oxygen demand as a function of flow velocity has been developed. Oxygen consumption in the sediment is modeled to be the sum of the biological (bacterial) consumption and the chemical consumption. The biological reaction is formulated by Michaelis-Menten kinetics and the chemical reaction is assumed to be a first-order reaction of dissolved oxygen.

The effect of the diffusive boundary layer in the water above the sediment on the SOD is shown quantitatively. This model suggests that, at very low velocity, the SOD is completely determined by the transport through the diffusive boundary layer and can simply be expressed in terms of velocity, DO concentration in the bulk water and a friction coefficient at the sediment surface. At higher velocity, the transport through the boundary layer is so fast that the processes in the sediment become rate limiting. In this case, the SOD is not affected by velocity but by biological and chemical oxygen consumption, apparent diffusion coefficient of oxygen in the sediment and the dissolved oxygen concentration. At intermediate velocity, the SOD is an increasing function of velocity and is also dependent on the sediment parameters. The above complex dependence of SOD on flow velocity is the most likely cause for the large divergence of SOD measurements often reported in the literature even for uniform and homogeneous sediments (Cerco at al. 1992). The velocity dependence of SOD through the boundary layer

thickness agrees with the observations by Belanger (1981) and Boynton et al. (1985). Predicted profiles of DO concentration in the boundary layer and in the sediment reproduce the observed profiles using microelectrodes (e.g. Joergensen and Revsbech, 1985).

The model also includes a dependence between the bulk DO concentration in the water and SOD. SOD is an increasing function of DO concentration and velocity. However, there is no upper limit of SOD when DO concentration becomes large, regardless of the value of the half saturation constant.

The model has been combined with a linear theory of the internal seiche motion in a rectangular, two-layered "lake" basin. The SOD averaged over a seiche motion is expressed in terms of wind velocity, the vertical position of the thermocline and the aspect ratio of the lake (fetch/water depth) as well as the oxygen consumption in the sediment. The average SOD is a monotonously increasing function of wind velocity and basin aspect ratio, but has an upper limit when these parameters are large enough. The average SOD is also sensitive to the position of the thermocline. It has a minimum value when the thermocline lies at the depth of 1/4 of the total depth.

APPENDIX I. Behavior of C_w, δ_s and δ_c as a function of U_* (see Fig.1 for definitions)

1. C_w Function

From Eqs. (21) and (29)

$$\frac{C_w}{C_\infty} = 1 - \frac{SOD}{fu_\infty C_\infty} = 1 - 2\frac{SOD_*}{U_*} \tag{A1}$$

For the special case that $Ko_{2*}=0$, SOD_*/U_* is a function of U_* and k'_* as:

$$\frac{SOD_*}{U_*} = \frac{k'_*+1}{2k'_*+1+\sqrt{(k'_*+1)U_*^2+1}} \tag{A2}$$

therefore,

$$\frac{C_w}{C_\infty} = 1 - \frac{2k'_*+2}{2k'_*+1+\sqrt{(k'_*+1)U_*^2+1}} = \frac{-1+\sqrt{(k'_*+1)U_*^2+1}}{2k'_*+1+\sqrt{(k'_*+1)U_*^2+1}} \tag{A3}$$

In the limit of $Ko_{2*}\to\infty$, $SOD_*\to\sqrt{k'_*}U_*/(U_*+2\sqrt{k'_*})$. Therefore,

$$\lim_{Ko_{2*}\to\infty}\frac{C_w}{C_\infty} = 1 - \frac{2\sqrt{k'_*}}{U_*+2\sqrt{k'_*}} = \frac{U_*}{U_*+2\sqrt{k'_*}} \tag{A4}$$

Fig. 5 shows C_w/C_∞ with varying Ko_{2*} and k'_* as well as U_*.

2. δ_s Function

Bouldin's analysis shows that δ_s is expressed as:

$$\delta_s = \sqrt{2D_s C_w / R} \qquad (A5)$$

Non-dimensional depth of the aerobic layer is expressed as:

$$\delta_{s*} = \frac{\delta_s}{\sqrt{2D_s C_\infty / \mu}} = \left[\frac{1}{Ko_{2*}+1-2SOD_*/U_*} + k'_* \right]^{-1/2} \qquad (A6)$$

For the special case that $Ko_{2*}=0$, SOD_*/U_* is written as Eq. (A2), then

$$\delta_{s*} = \left[\frac{2k'_*+1+\sqrt{(k'_*+1)U_*^2+1}}{-1+\sqrt{(k'+1)U_*^2+1}} + k'_*\right]^{-1/2} = \frac{U_*}{1+\sqrt{(k'_*+1)U_*^2+1}} \qquad (A7)$$

Eq. (A6) shows that in the general case of $Ko_{2*} \neq 0$, δ_{s*} has a non-zero limit as $U_* \to 0$, since $SOD_* \to 1/2U_*$. Therefore,

$$\lim_{U_* \to 0} \delta_{s*} = \left[\frac{1}{Ko_{2*}} + k'_* \right]^{-1/2} = \sqrt{\frac{Ko_{2*}}{1+k'_* Ko_{2*}}} \qquad (A8)$$

The other limit at large velocity is

$$\lim_{U_* \to \infty} \delta_{s*} = \left[\frac{1}{Ko_{2*}+1} + k'_* \right]^{-1/2} = \sqrt{\frac{Ko_{2*}+1}{1+k'_*(Ko_{2*}+1)}} \qquad (A9)$$

When reactions in the sediments are all first order reactions of DO, flow velocity does not affect δ_s so that δ_s remains constant.

In the limit $Ko_{2*} \to \infty$,

$$\lim_{Ko_{2*} \to \infty} SOD_* = \sqrt{k'_* U_* / (U_* + 2\sqrt{k'_*})} \qquad (A10)$$

Therefore,

$$\lim_{Ko_{2*}\to\infty} \delta_{s*} = \left[\frac{1}{Ko_{2*}+1-\dfrac{2\sqrt{k'_*}}{U_*+2\sqrt{k'_*}}} + k'_* \right]^{-1/2} \qquad (A11)$$

See Figs. 6 and 7, which show δ_{s*} as a function of Ko_{2*} and k'_*.

3. δ_c Function and DO Concentration Profile

It is useful to define a mass transfer coefficient, k_A, as

$$k_A = SOD/(C_\infty - C_W) = f(C_f, S_c)u_\infty \qquad (A12)$$

If we use Deissler's formula (21), k_A is expressed as

$$k_A = \frac{2}{\pi} n\sqrt{C_f} S_c^{-3/4} u_\infty \qquad (A13)$$

The thickness of the effective boundary layer, δ_c, can be defined as

$$\delta_c = D/k_A \qquad (A14)$$

Substituting Eq. (A13) into Eq. (A14),

$$\delta_c = \frac{D}{f(C_f, S_c)u_\infty} = \frac{(\nu^3 D)^{1/4}}{\frac{2}{\pi} n\sqrt{C_f} u_\infty} \qquad (A15)$$

δ_c is not dependent on biological and chemical reaction parameters but on physical parameters of the water. This equation can be non-dimensionalized as follows:

$$\delta_{c*} = \frac{\delta_c}{\sqrt{2D_s C_\infty/\mu}} = \frac{D}{D_s U_*} \tag{A16}$$

With Eqs. (19) and (16), DO concentration distribution can be calculated as

$$\int_{C_w}^{C} dC = \int_{0}^{y} \frac{SOD/\nu}{(1/S_c)+(nu_*/\nu)^4 y^4}\, dy \tag{A17}$$

Non-dimensionalized concentration C^+ is then expressed as

$$C^+ = \frac{C(y)-C_w}{C_\infty - C_w}$$

$$= \frac{1}{2\Pi}\left[\ln\left|\frac{y^{+2}+\sqrt{2}qy^{+}+q^2}{y^{+2}-\sqrt{2}qy^{+}+q^2}\right| + 2\arctan\left(\frac{\sqrt{2}qy}{q^2-y^{+2}}\right) \right] \tag{A19}$$

where

$$q = S_c^{-1/4} n^{-1} \tag{A20}$$

APPENDIX II. REFERENCES

Belanger, B.T. (1981). "Benthic oxygen demand in Lake Apopka, Florida." Water Research, 15, 267-274.

Berelson, W.M., and Hamond, D.E. (1990). "Sediment oxygen demand measurements using benthic flux chambers." in Cerco et al. (1992), 153-167.

Bouldin, D.R. (1968). "Methods for describing the diffusion of oxygen and other mobile constituents across the mud-water interface." J. Ecology, 56, 77-87.

Boynton, W.R., Kemp, W.M., Osborne, C.G., Kaumeyer, K.R., and Jenkins, M.C. (1981). "Influence of water circulation rate on in situ measurements of benthic community respiration." Marine Biology, 65, 185-190.

Burns, N.M. (1970). "Oxygen depletion in the central and eastern basins of Lake Erie." Journal of Fish. Res. Bd. Canada, 33, 512-519.

Cerco, C., Gunnison, D., and Price, C.B. (1992). Proceedings, US Army Corps of Engineers Workshop on Sediment Oxygen Demand, Providence, Rhode Island 21-22 August 1990, Miscellaneous Paper W-92-1, Environmental Laboratory, Waterways Experimental Station, Corps of Engineers, Vicksburg, MS.39180-6199, June, 186pp.

Dale, T. (1978). "Total chemical and biological oxygen consumption of the sediment in Lindaspollene, Western Norway." Marine Biology, 49, 333-341.

Davis, W.S., and Hendendorf, C.E. (1986). "Regression analysis of Lake Erie's sediment oxygen demand." Sediment Oxygen Demand. Processes, modeling and measurement. K.J. Hatcher ed., University of Georgia Press, Athens, Ga., 235-238.

Dawson, D.A., and Trass, O. (1972). "Mass transfer at rough surfaces." International Journal of Heat and Mass Transfer, 15, 1317-1336.

Deissler, R.G. (1951). "Investigation of turbulent flow and heat transfer in smooth tubes, including the effects of variable fluid properties." Trans. ASME., 73(1), 101-105.

Deissler, R.G. (1954). "Heat transfer and fluid friction for fully developed turbulent flow of air and supercritical water with variable fluid properties." Trans. ASME., 76(1), 73-86.

Di Toro, D.M., Paquin, P.R., Subburamu, K., and Gruber, D.A. (1990). "Sediment oxygen demand model: Methane and ammonia oxidation." J. Envir. Engrg., ASCE, 116(5), 945-986.

Eckert, E.R.G. and Drake Jr. R.M. (1972). "Analysis of Heat and Mass Transfer", McGraw Hill, New York, 806pp.

Edwards, R.W., and Rolley, H.L.J. (1965). "Oxygen consumption of river muds." J. Ecology, 53(1), 1-19.

Ellis, C.R., and Stefan, H.G. (1989). "Oxygen demand in ice covered lakes as it pertains to winter aeration." Water Resources Bulletin, 25(6), 1169-1176.

Gundersen, J.K., and Joergensen, B.B. (1990). "Microstructure of diffusive boundary layers and the oxygen uptake of the sea floor." Nature, 345, 604-607.

Hall, P.O.J., Anderson, L.G., Rutgers van der Loeff, M.M., Sundby, B., and Westerlund, S.F.G. (1989). "Oxygen uptake kinetics in the benthic boundary layer." Limnology and Oceanography, 34(4), 734-746.

Hanes, N.B., and Irvine, R.L. (1968). "New techniques for measuring oxygen uptake rates of benthic systems." J. Water Pollut. Control Fed., 40, 223-232.

Hargrave, B.T. (1973). "Coupling carbon flow through some pelagic and benthic communities." J. Fish. Res. Bd. Canada, 30, 1317-1326.

Hicks, D.B. (1990). "EPA Region IV perspective on SOD." in Cerco et al. (1992), 110-119.

Janke, R.A. (1990). "Chamber measurements of benthic metabolism: Insights from deep seafloor studies." in Cerco et al. (1992), 120-136.

Joergensen, B.B., and Des Marais, D.J. (1990). "The diffusive boundary layer of sediments: Oxygen microgradients over a microbial mat." Limnology and Oceanography, 35(6), 1343-1355.

Joergensen, B.B., and Fenchel, T. (1974). "The sulfur cycle of a marine sediment model system. Marine Biology, 24, 189-201.

Joergensen, B.B., and Revsbech, N.P. (1985). "Diffusive boundary layers and oxygen uptake of sediments and detritus." Limnology and Oceanography, 30(1), 111-122.

Karman, T.von. (1939). "The analogy between fluid friction and heat transfer," Transactions, ASME, 61, 705-710.

Katto, Y. (1964). "An introduction to heat transfer." Yokendo, Tokyo.

Mathias, J.A., and Barica, J. (1980). "Factors controlling oxygen depletion in ice-covered lakes." Can. J. Fish. Aqua. Sci., 37, 185-194.

Monin, A.S., and Yaglom, A.M. (1965). "Statistical Fluid Mechanics." The M.I.T. Press, Cambridge, Mass.

Officer, C.B., Biggs, R.B., Taft, J.T., Cronin, L.E., Tyler, M.A., and Boynton, W.R. (1984). "Chesapeake Bay anoxia: Origin, development and significance." Science, 223, 22-27.

Polak, J., and Haffner, G.D. (1978). "Oxygen depletion of Hamilton Harbour." Water Research, 12(4), 205-215.

Prandtl, L. (1910). "Eine Beziehung Zwischen Waermeaustausch und Stroemungswiderstand der Flussigkeiten." Phys. Zeitschr., 11, 1072-1078.

Riley, M.J., and Stefan, H.G. (1988). "MINLAKE: A dynamic lake water quality simulation model." Ecological Modelling, 43, 155-182.

Shaw, D.A., and Hanratty, T.J. (1977). "Turbulent mass transfer rates to a wall for large Schmidt numbers." AIChE Journal, 23(1), 28-37.

Shirozuka, T., Hirata, A., and Murakami, A. (1966). "Transport phenomena for chemical engineers." Ohm-Sha, Tokyo.

Stefan, H.G. (1990). "Sediment oxygen demand and its effect on winterkill in lakes." in Cerco et al. (1992), 137-142.

Taylor, G.I. (1916). "Conditions at the surface of a hot body exposed to the wind." Brit. Adv. Com. Aero. Rep. and Memor., 272, 423

Thomann, R.V. and Mueller, J.A. (1987). Principles of Surface Water Quality Modeling and Control, Harper International Edition.

Turner, J.S. (1973). "Buoyancy effects in fluids." Cambridge University Press, Cambridge.

Walker, R.R., and Snodgrass, W.J. (1986). "Model for sediment oxygen demand in lakes." J. Envir. Engrg., ASCE, 112(1), 25-43.

Whittemore, R.C. (1990). "Studies on the comparison of in-situ and laboratory sediment oxygen demand measurement techniques." in Cerco et al. (1992), 100-109.

Zobell, C.E. (1943). "Bacterial utilization of low concentration of organic matter." Journal of Bacteriology, 45, 555-564.

Zobell, C.E., and Brown, F. (1944). "Studies on the chemical preservation of water samples." Journal of Marine Research, 5(3), 178-184.

APPENDIX III. NOTATION

The following symbols are used in this paper:

A = $\sqrt{1+bHC_\infty(0)}$;

B = $\sqrt{1+bHC_\infty(t)}$;

a = $2fu_\infty/H$ (s^{-1});

b = $2f^2u_\infty^2/D_s\mu H$ (m^2/gO_2);

C = dissolved oxygen concentration (gO_2/m^3);

C_f = friction coefficient;

C_ℓ = dissolved oxygen concentration at depth δ_ℓ (gO_2/m^3);

C_w = dissolved oxygen concentration at the sediment-water interface (gO_2/m^3);

C_∞ = dissolved oxygen concentration in the bulk water; (gO_2/m^3);

$\hat{C}_\infty$ = non-dimensional dissolved oxygen concentration in the bulk water (gO_2/m^3);

D = molecular diffusion coefficient for O_2 in pure water (m^2/s);

D_s = apparent diffusion coefficient for O_2 in interstitial water (m^2/s);

f = $\frac{2}{\pi}n\sqrt{C_f}S_c^{-3/4}$;

g = acceleration of gravity (m/s^2);

H = total depth of a lake (m);

h_1 = depth of the upper layer of a lake (m);

h_2 = depth of the lower layer of a lake (m);

h_* = non-dimensional depth of the lower layer;

J = flux of DO from sediment $(gO_2/m^2 day)$;

K_M = turbulent diffusivity for momentum (m^2/s);

Ko_2 = half saturation constant for O_2 (gO_2/m^3);

Ko_2* = non-dimensional half saturation constant for O_2;

$\hat{Ko}_2$ = non-dimensional half saturation constant for O_2;

K_y = turbulent diffusivity for mass (m^2/s);

k = 0.36;

k_A = mass transfer coefficient (m/s);

k' = first-order reaction rate constant (s^{-1});

k'* = non-dimensional first-order reaction rate constant;

$\hat{k}'$ = non-dimensional first-order reaction rate constant;

ℓ = fetch of a lake (m);

n = 0.109;

p = constant in SOD solution (s/m);

R = volumetric oxygen consumption rate ($gO_2/m^3 day$);

r = ratio of chemical and biological reaction rate;

S_c = Schmidt number for O_2;

S_{ct} = turbulent Schmidt number for O_2;

SOD = flux of O_2 to sediment ($gO_2/m^2 day$);

SOD_* = non-dimensional flux of O_2 to sediment;

$\bar{\bar{SOD}}$ = time and space averaged flux of O_2 to sediment ($gO_2/m^2 day$);

$\bar{\bar{SOD}}_*$ = non-dimensional, time and space averaged flux of O_2 to sediment;

$\hat{SOD}$ = non-dimensional flux of O_2 to sediment;

t = time (s);

T = period of seiche motion (s);

u_ℓ = velocity at depth δ_ℓ (m/s);

u_{max} = maximum velocity due to seiche motion (m/s);

u_* = shear velocity (m/s);

u_∞ = velocity out of the boundary layer (m/s);

u^+ = non-dimensional velocity;

U_* = non-dimensional velocity;

W = wind velocity (m/s);

x = horizontal coordinate along the fetch (m);

y = vertical coordinate, positive upward, from the sediment water interface (m);

y^+ = non-dimensional velocity;

δ_c = thickness of the effective boundary layer (m);

δ_ℓ = thickness of the laminar sublayer (m);

δ_s = depth of the aerobic zone (m);

δ_s* = non-dimensional depth of the aerobic zone;

ε = relative density of water;

κ = wave number of seiche (m^{-1});

μ = maximum aerobic oxidation rate (gO_2/m^3 day);

ν = kinematic viscosity (m^2/s);

ρ = density of water (g/m^3);

ρ_1 = density of the upper layer of a lake (g/m^3);

ρ_2 = density of the lower layer of a lake (g/m^3);

σ = angular frequency (s^{-1});

τ = shear stress (N/m^2);

τ_w = shear stress applied at the water surface (N/m^2); and

τ_* = windshear function.

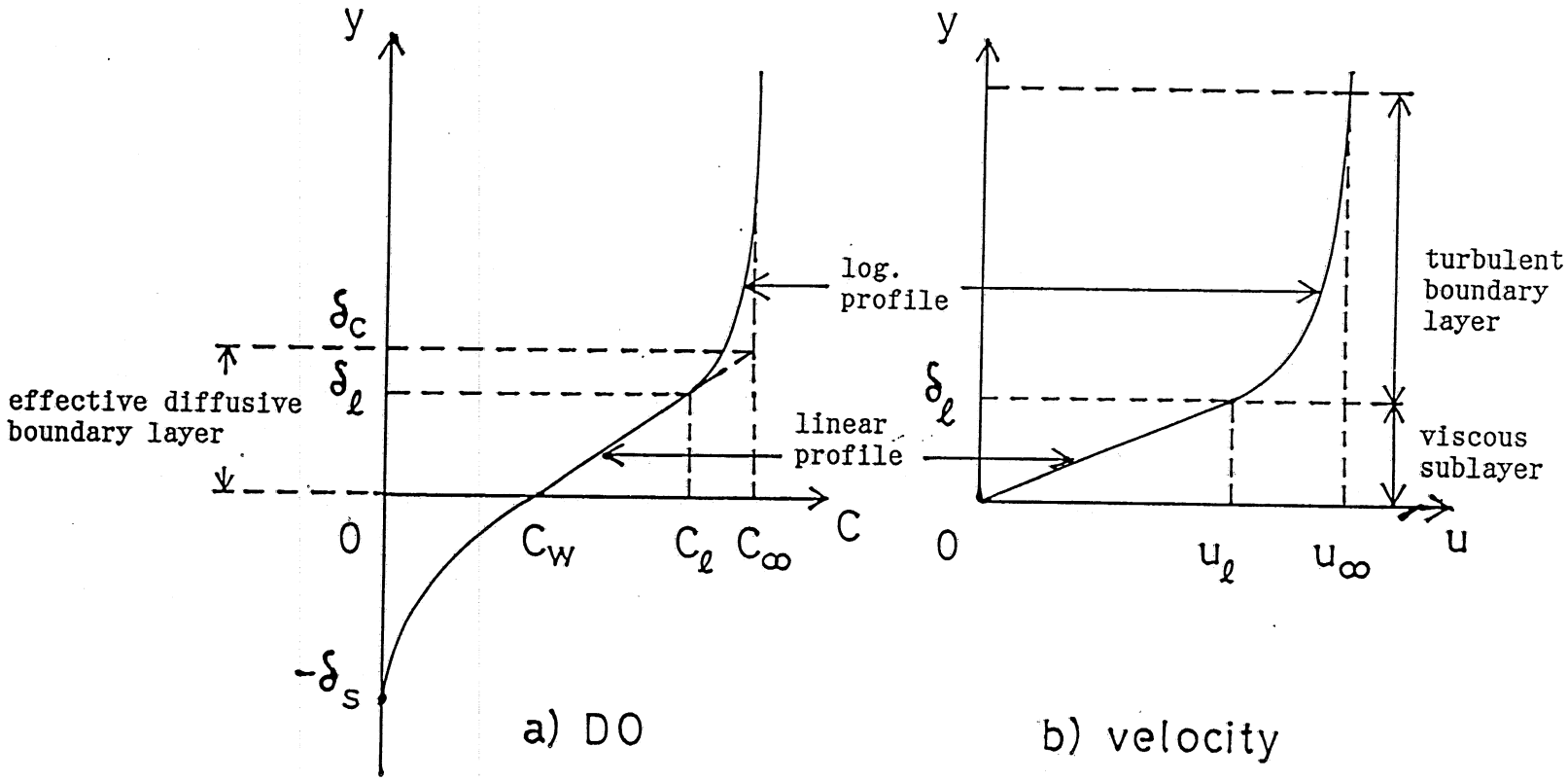

Fig. 1 Schematic distribution of dissolved oxygen concentration (a) and flow velocity (b). The boundary layer is divided into a viscous sublayer and the turbulent layer.

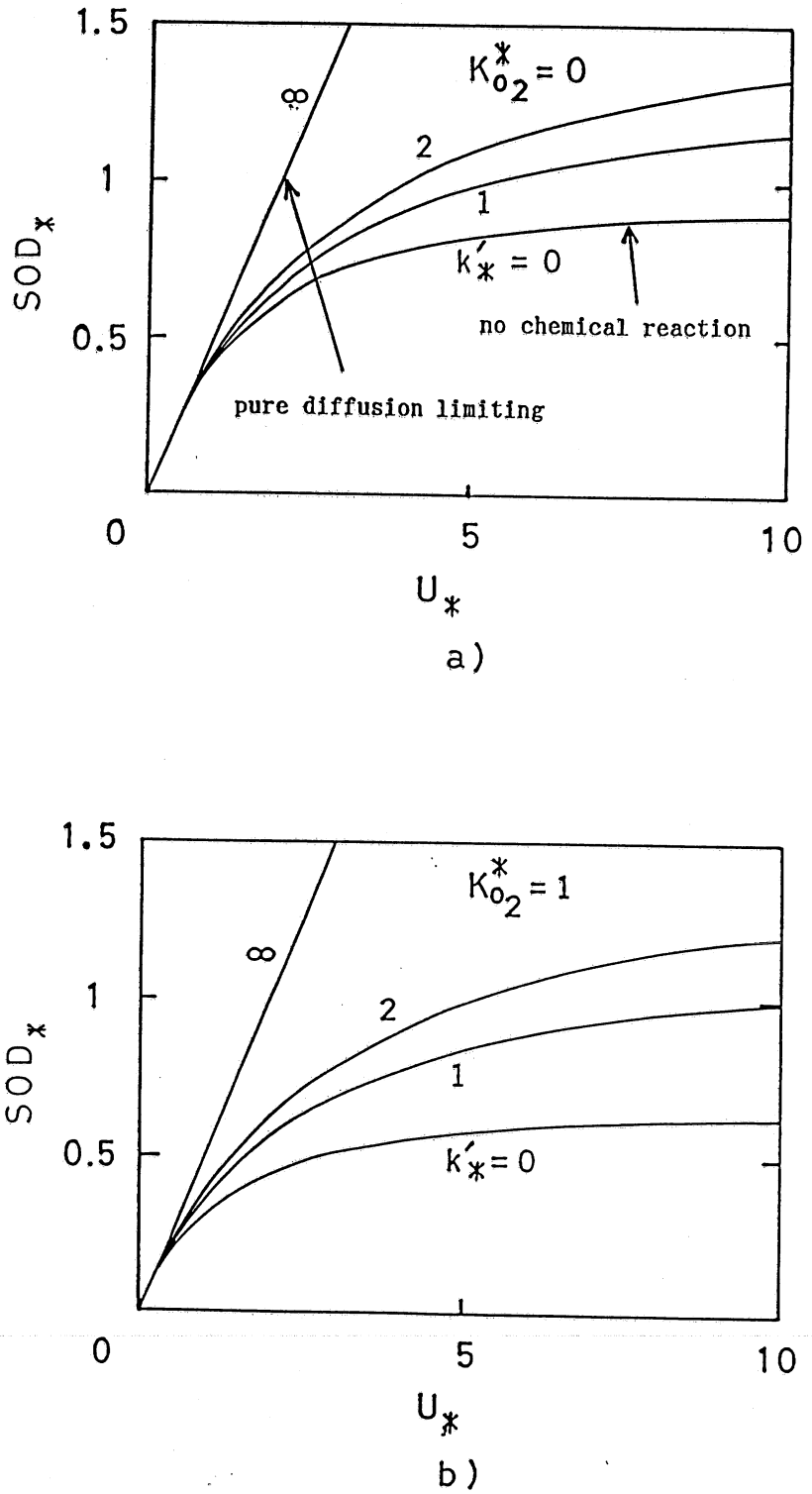

Fig. 2. Non–dimensional, sediment oxygen demand (SOD) as function of non–dimensional velocity and first–order reaction rate constant k_*'; (a) $K_{02*}=0$; (b) $K_{02*}=1$. (Defined in Eqs. 25 and 27)

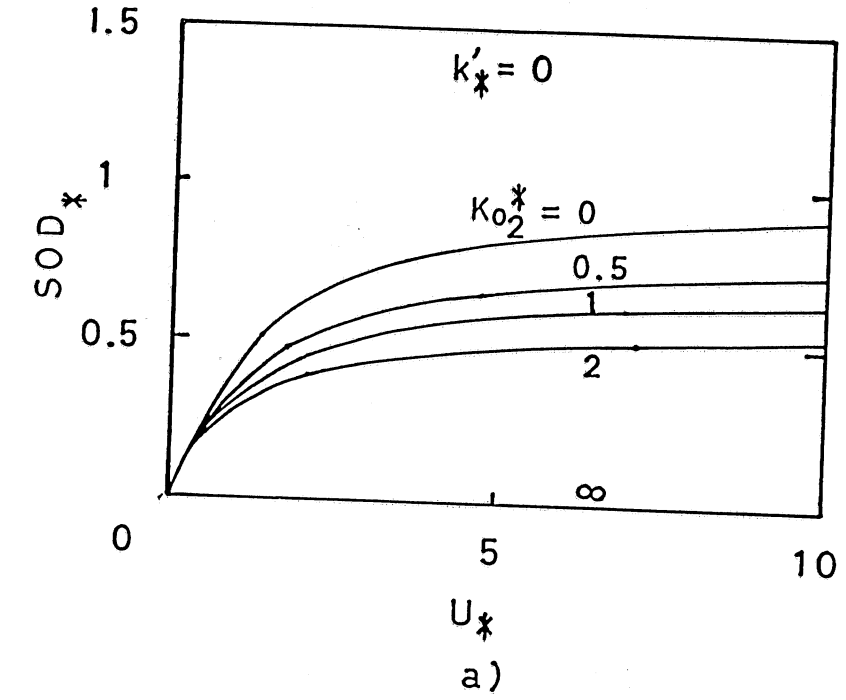

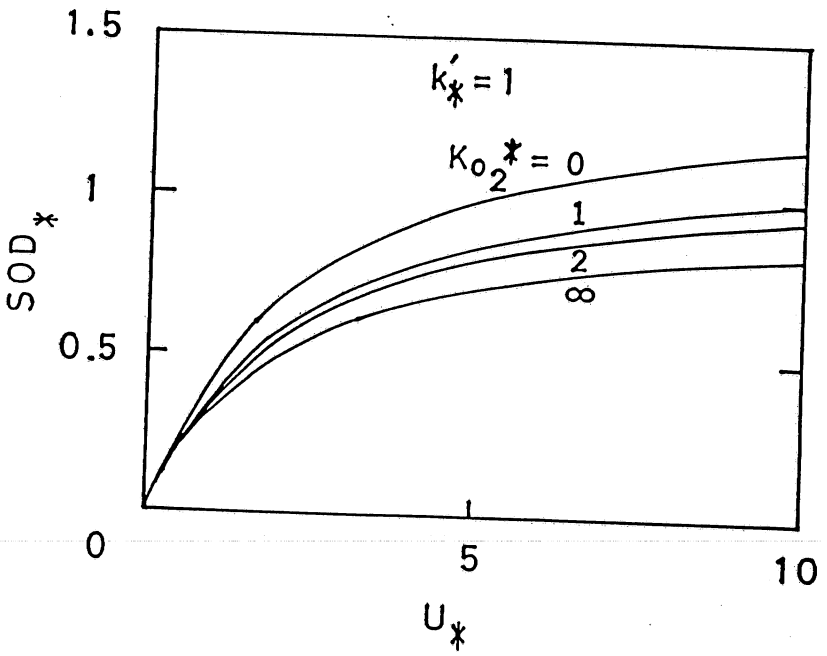

Fig. 3. Non–dimensional, sediment oxygen demand (SOD) as function of non–dimensional velocity and half saturation constant K_{02*}: (a) $k_*'=0$; (b) $k_*'=1$.

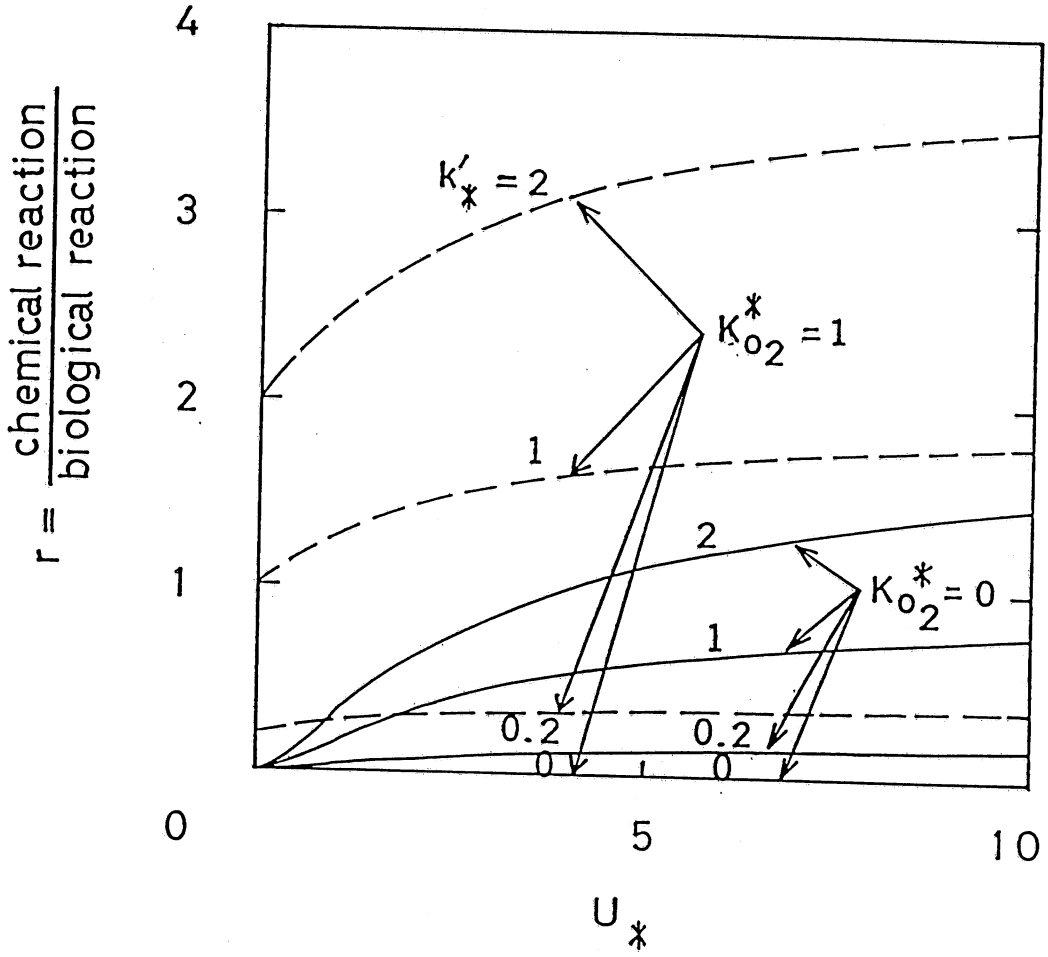

Fig. 4. Ratio of chemical and biological reactions as function of non–dimensional velocity, K_{02*}, and k_*'.

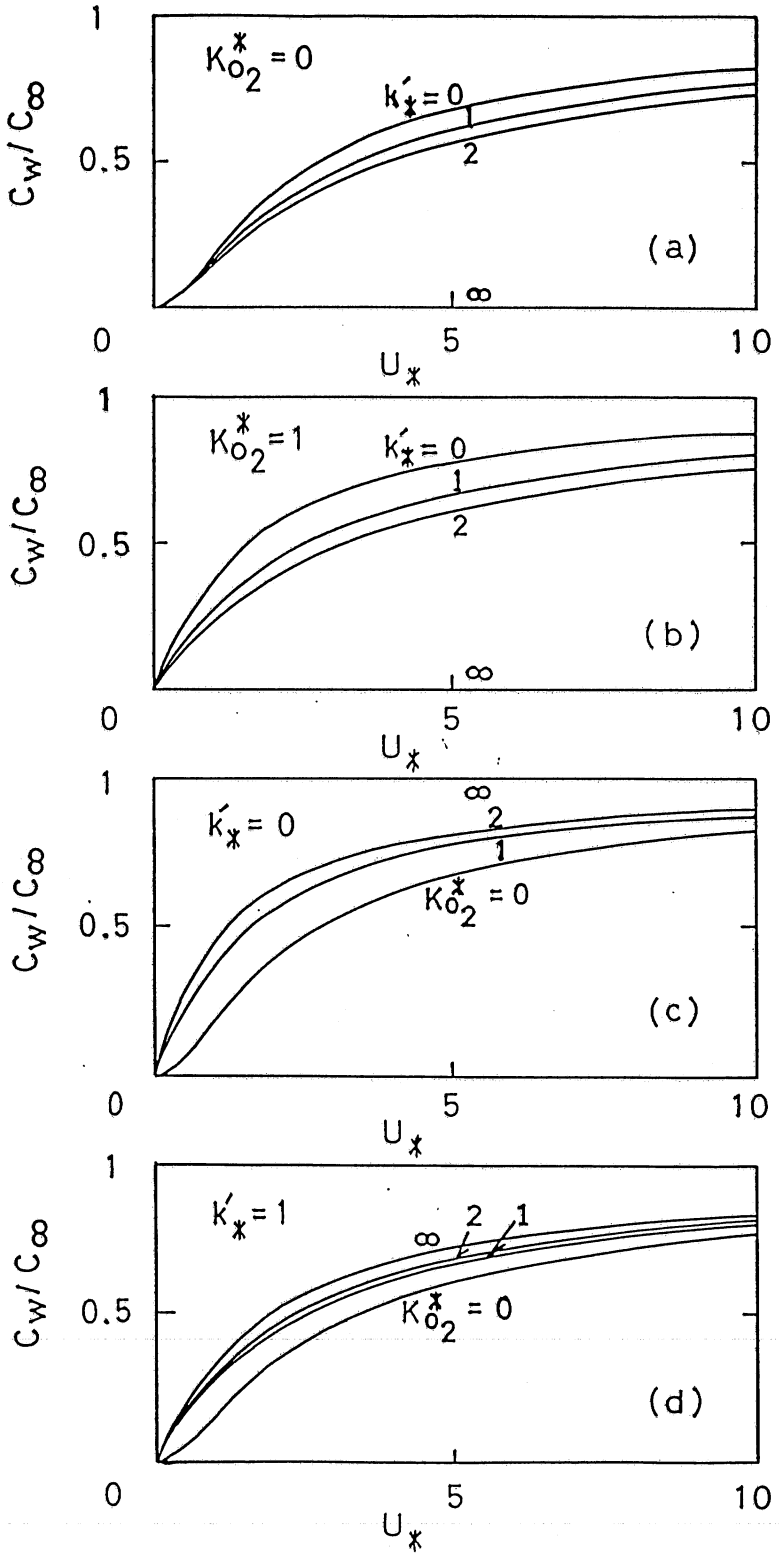

Fig. 5. Dissolved oxygen concentration at the sediment water interface as function of non–dimensional velocity, K_{02*} and k_*': (a) $K_{02*}=0$; (b) $K_{02*}=1$; (c) $k_*'=0$; (d) $k_*'=1$.

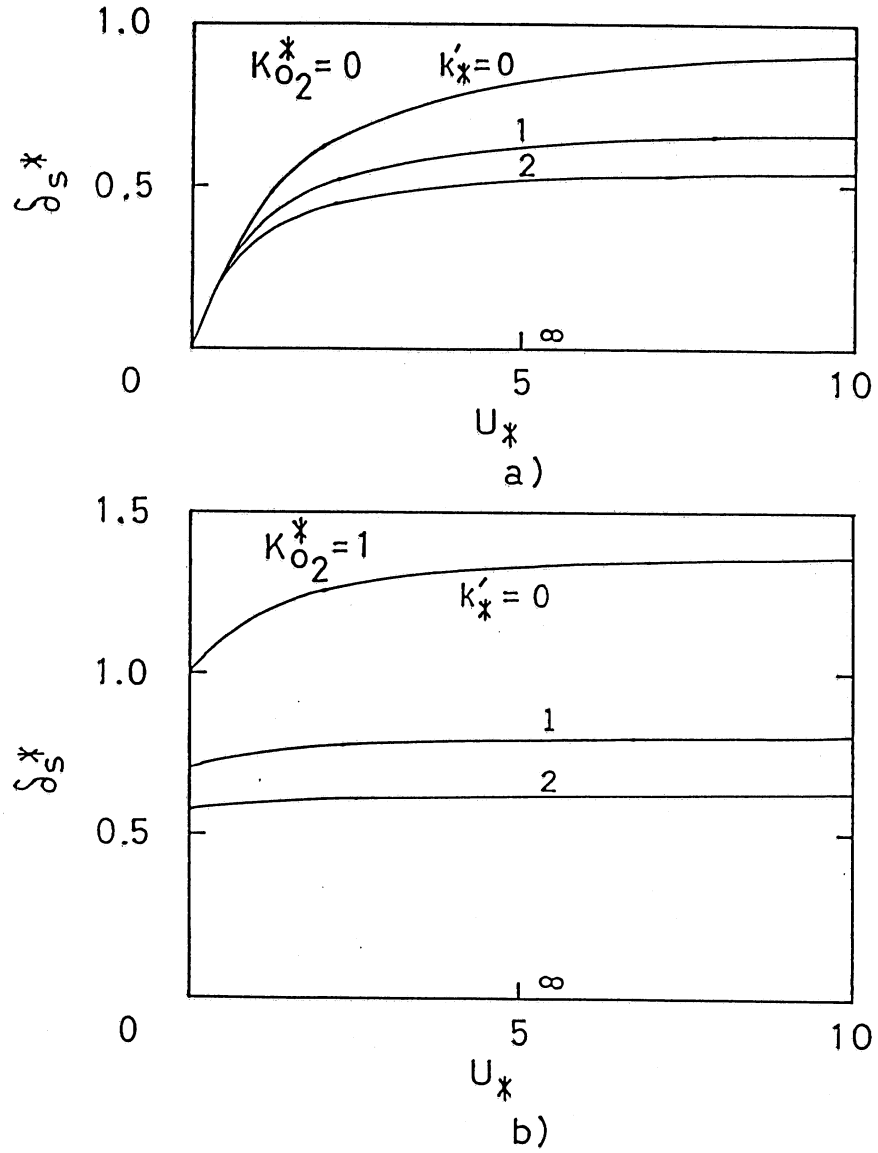

Fig. 6. Non–dimensional thickness of the aerobic zone in the sediment as function of non–dimensional velocity and first–order reaction rate constant k_*': (a) $K_{02*}=0$; (b) $K_{02*}=1$.

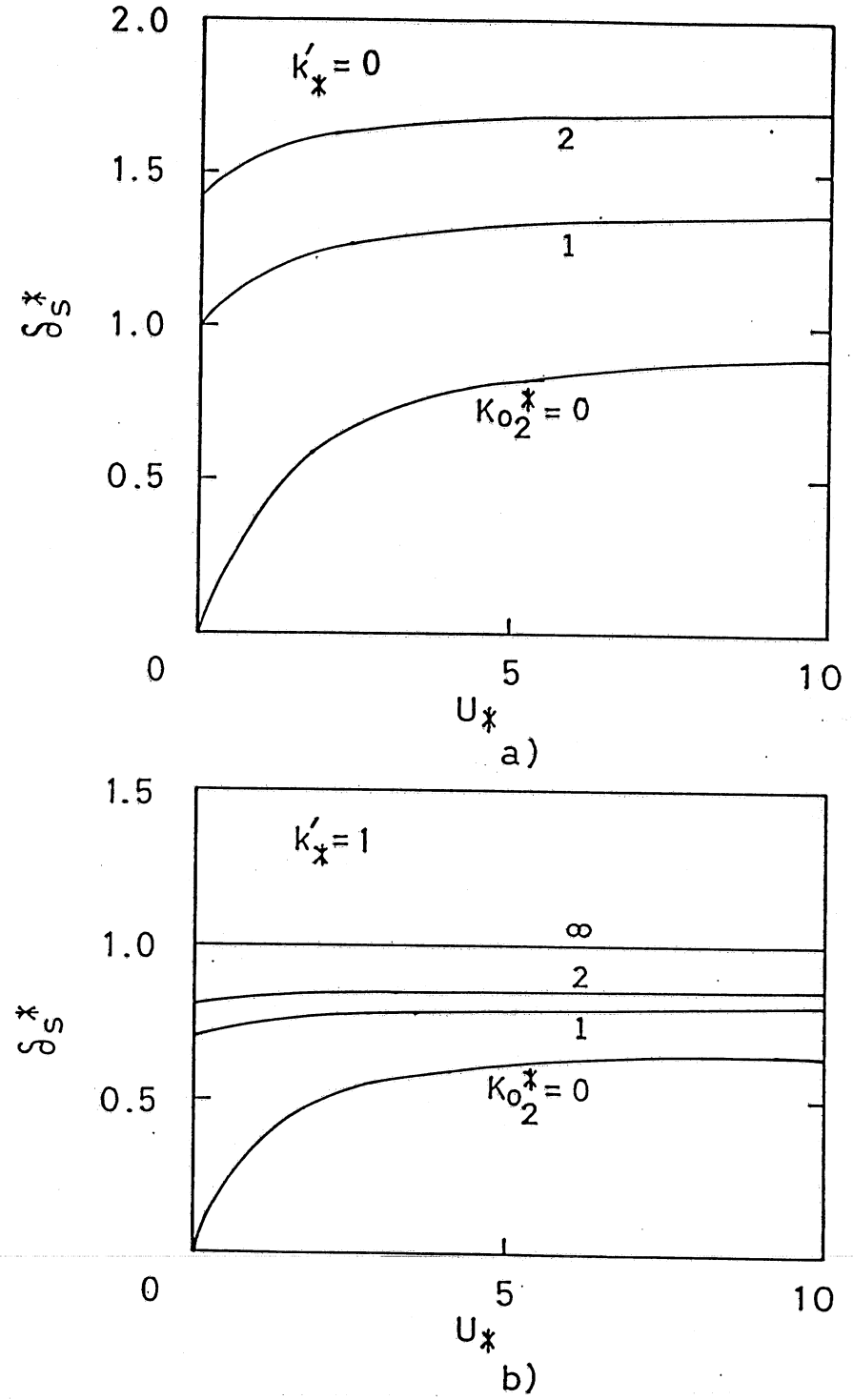

Fig. 7. Non–dimensional thickness of the aerobic zone in the sediment as function of non–dimensional velocity and a half saturation constant K_{02*}: (a) $k_*'=0$; (b) $k_*'=1$.

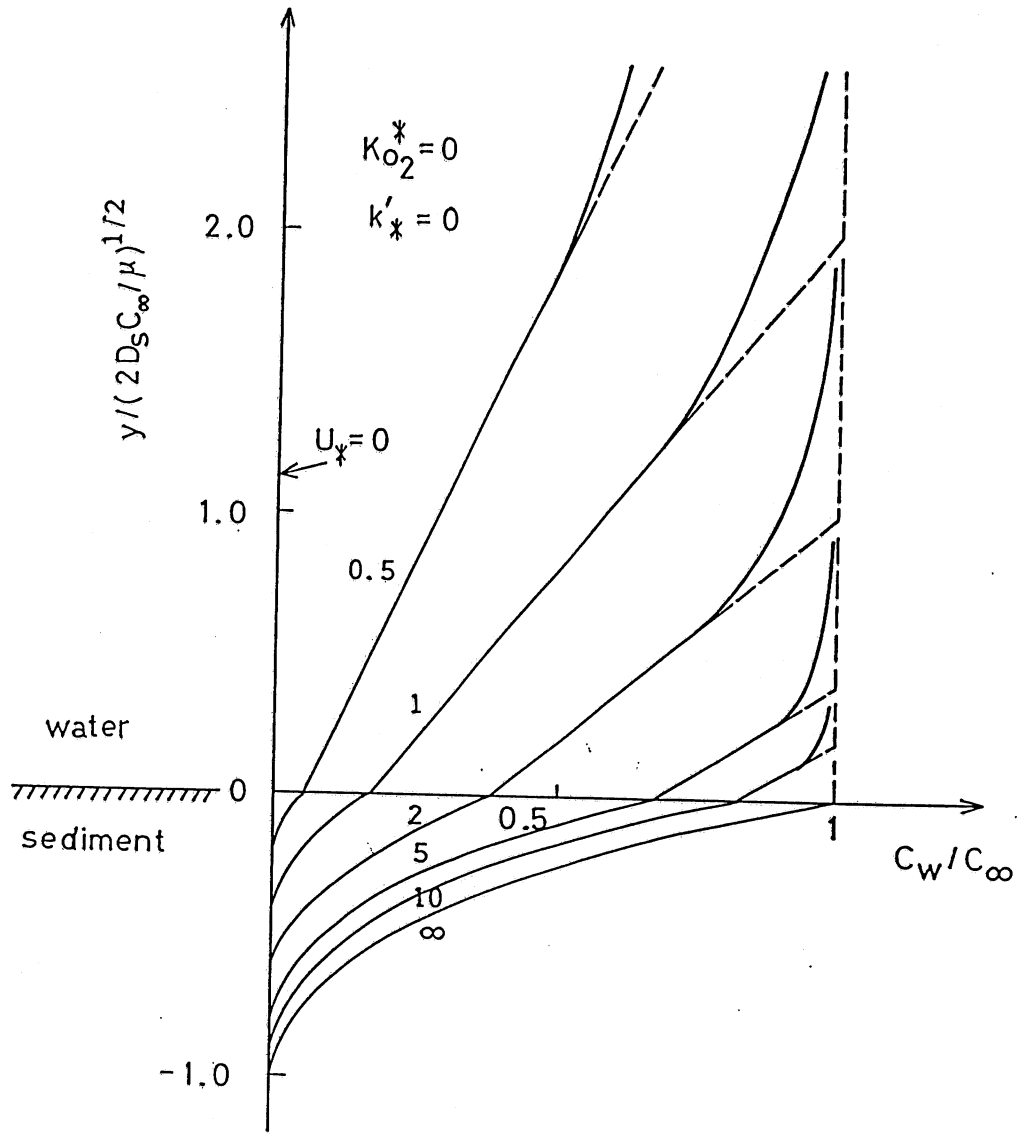

Fig. 8. Vertical distribution of dissolved oxygen concentration as function of non–dimensional velocity: $K_{02*}=0$ and $k_*'=0$.

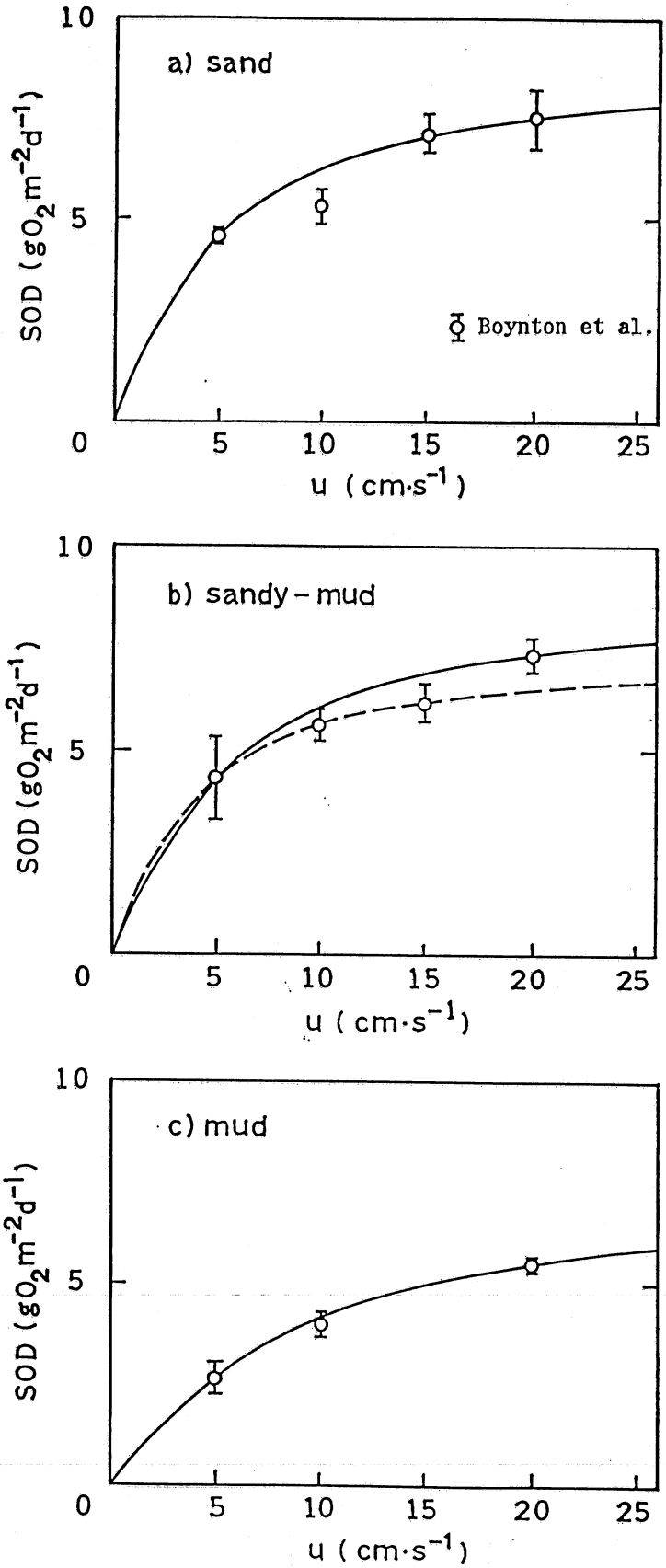

Fig. 9. Comparison of observed and calculated results of SOD as a function of velocity. Open circles denote measurements by Boynton et al. (1980) using an in situ chamber at three different sediments representing (a) sand, (b) sandy–mud and (c) mud environments. Estimated values of $(2D_s\mu C_\infty)^{1/2}$ and $(2f^2C_\infty/D_s\mu)^{1/2}$ are (a) 9.1 $gm^{-2}d^{-1}$ and 0.27 $cm^{-1}s$, (b) 9.0 $gm^{-2}d^{-1}$ and 0.25 $cm^{-1}s$ (7.5 and 0.35 for broken curve) and (c) 7.4 $gm^{-2}d^{-1}$ and 0.16 $cm^{-1}s$.

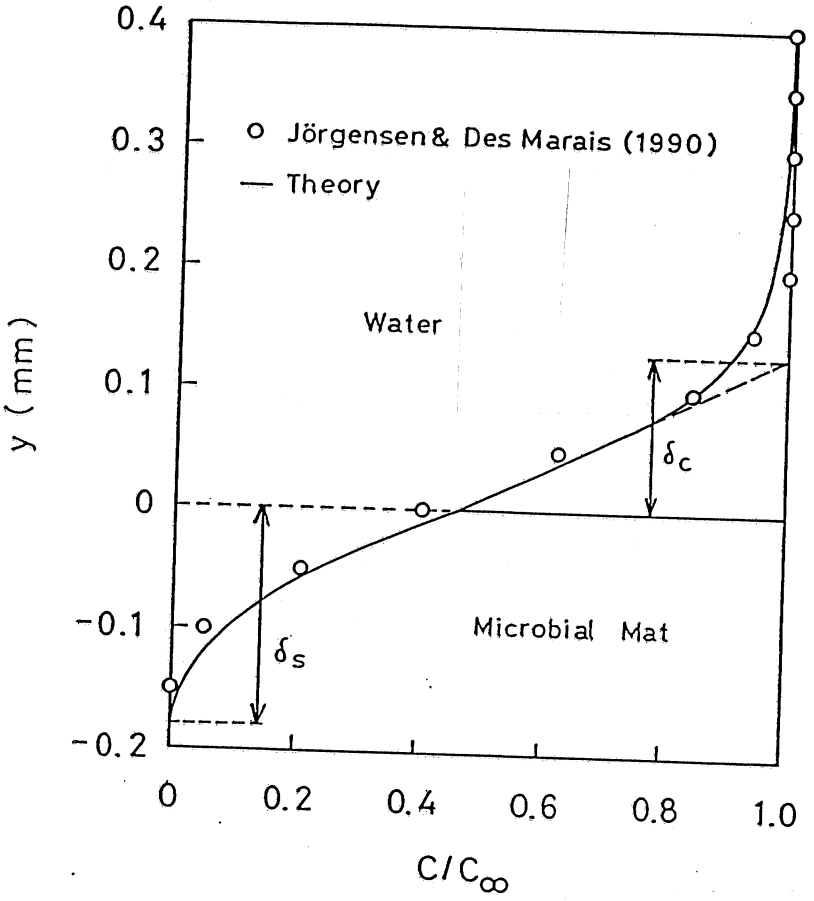

Fig. 10. Observed and calculated vertical distributions of dissolved oxygen concentrations. Open circles denote measurements by Joergensen and Des Marais (1990) in a laboratory experiment with a rough sediment—water interface (microbial mat) from a saline pond. The theoretical line is for a smooth wall and obtained by the theory given herein.

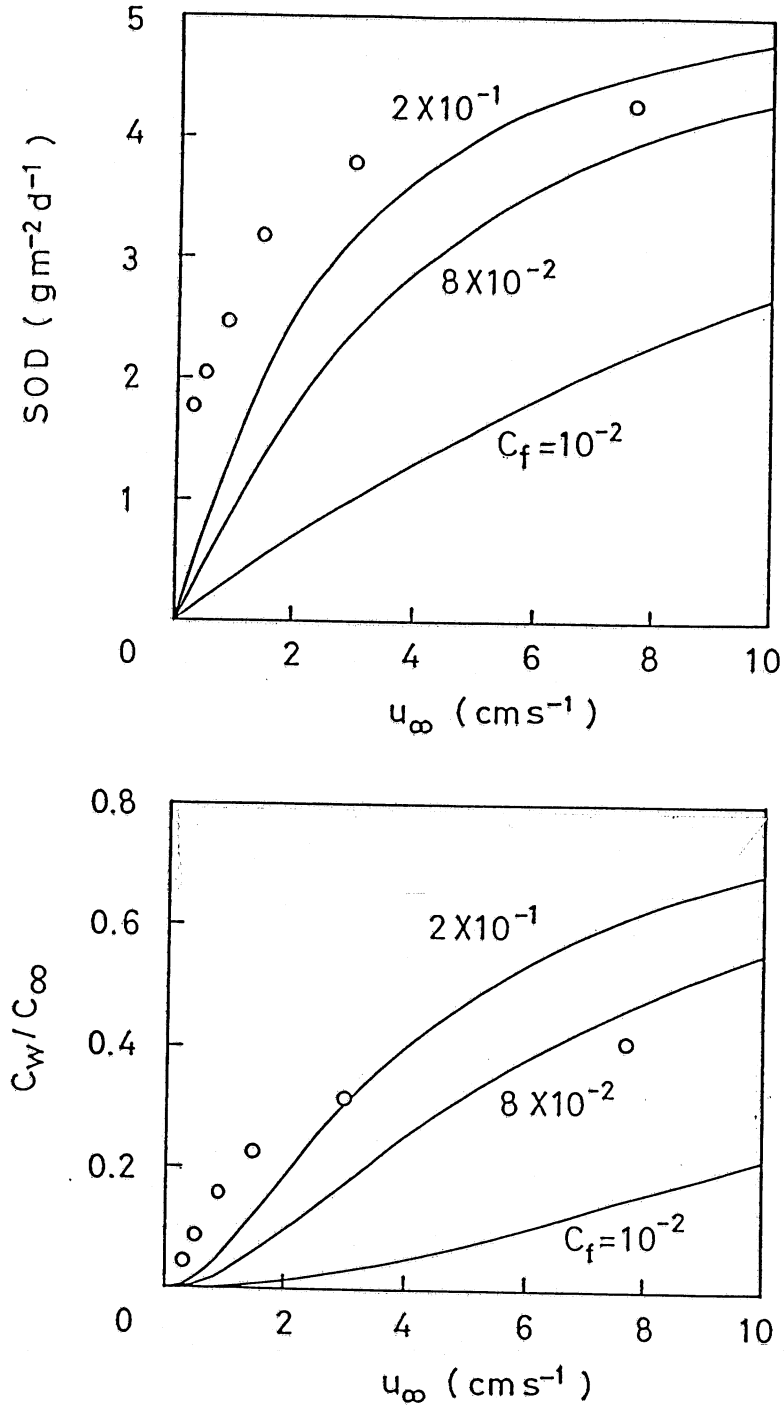

Fig. 11. Observed and calculated results of SOD as a function of velocity. Open circles denote measurements by Joergensen and Des Marais (1990) in a laboratory experiment with a sediment–water interface (microbial mat) from a saline pond. The theoretical lines are for a smooth wall and obtained by the theory given herein.

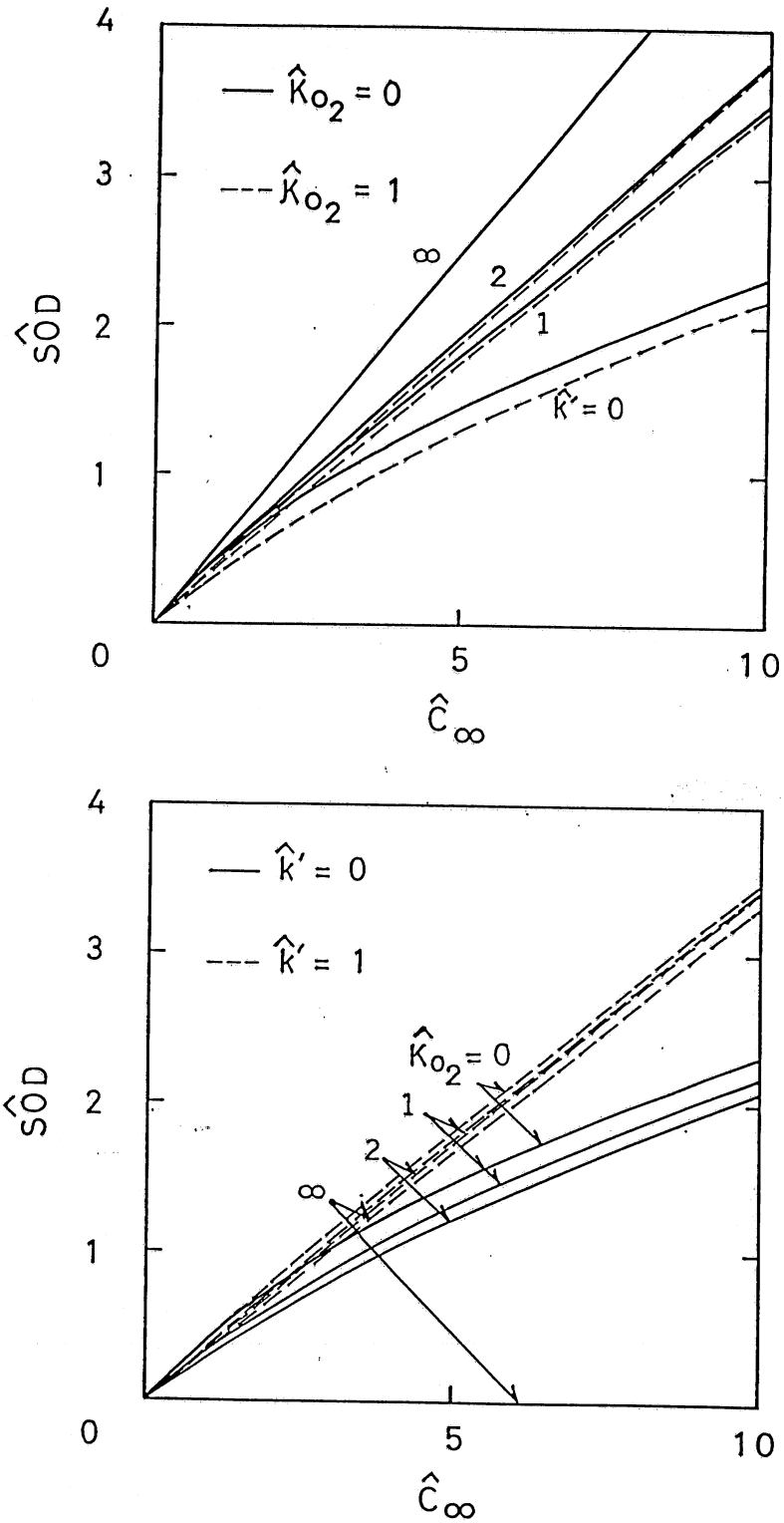

Fig. 12. Non–dimensional SOD as function of non–dimensional DO concentration and (a) first–order reaction rate constant k_*' and (b) half saturation constant K_{02*}.

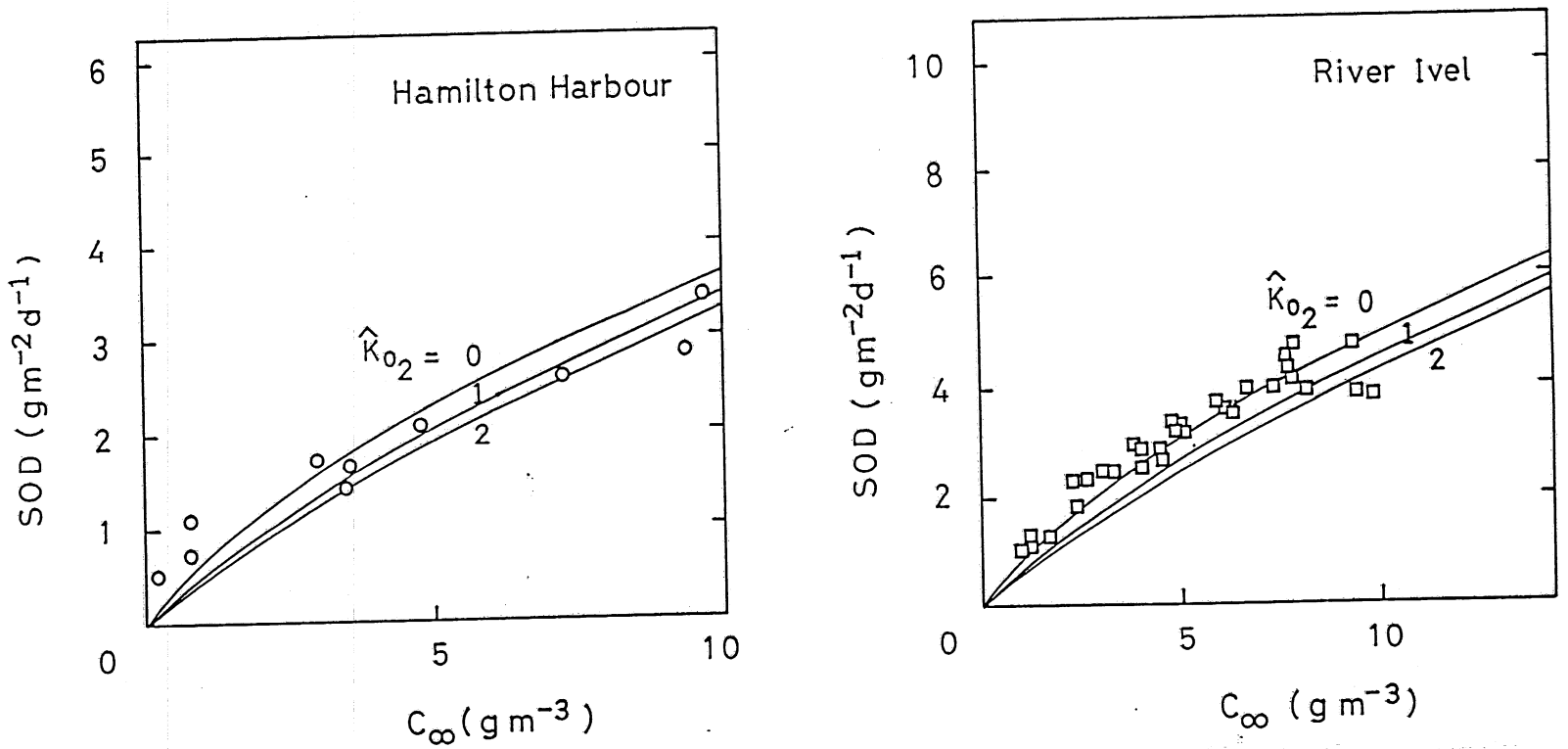

Fig. 13. Comparison of calculated and measured SOD as function of DO concentration; data from Polak and Haffner (1978) (left) and Edwards and Rolley (1965)(right).

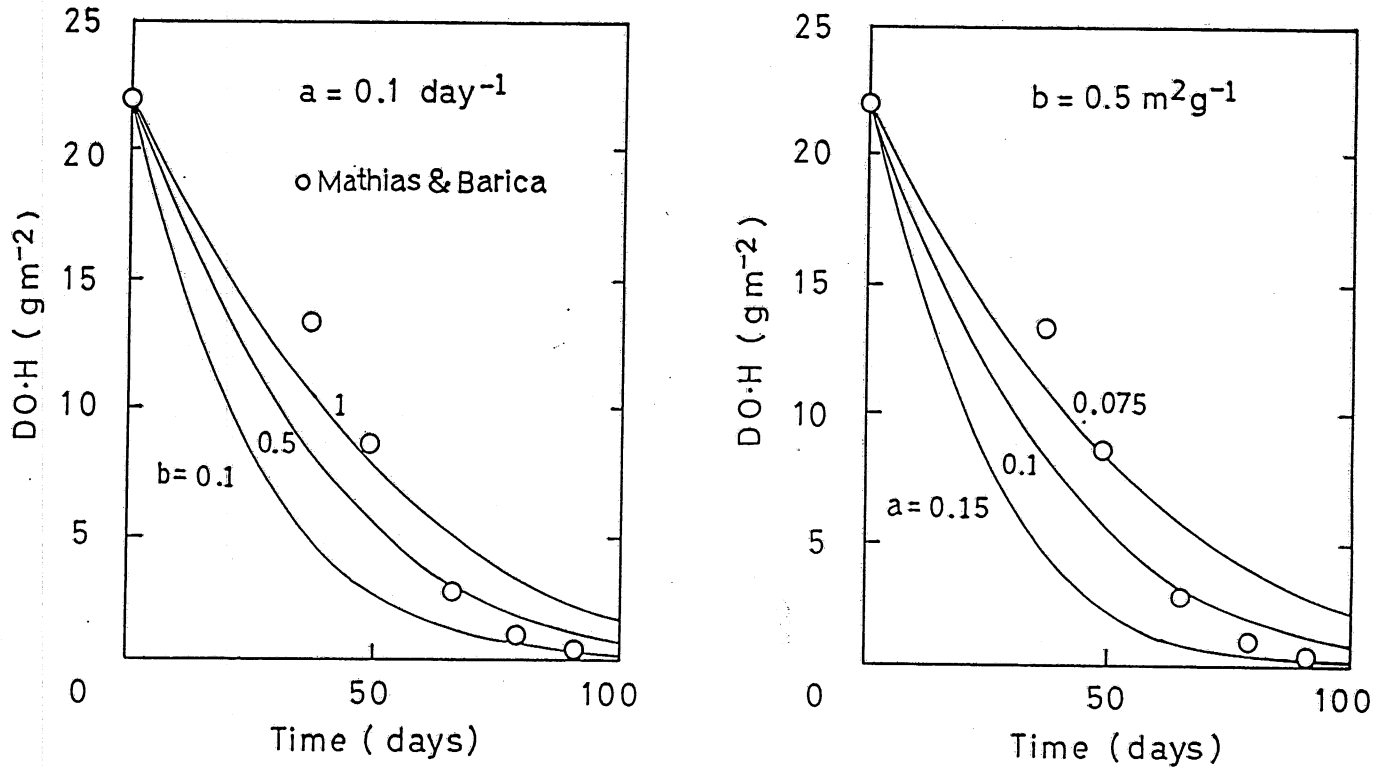

Fig. 14. Comparison of model predictions of DO concentration with measurements for an ice covered lake by Mathias and Barica (1980); left, a=0.1 day^{-1} right, b=0.5 m^2g^{-1}.

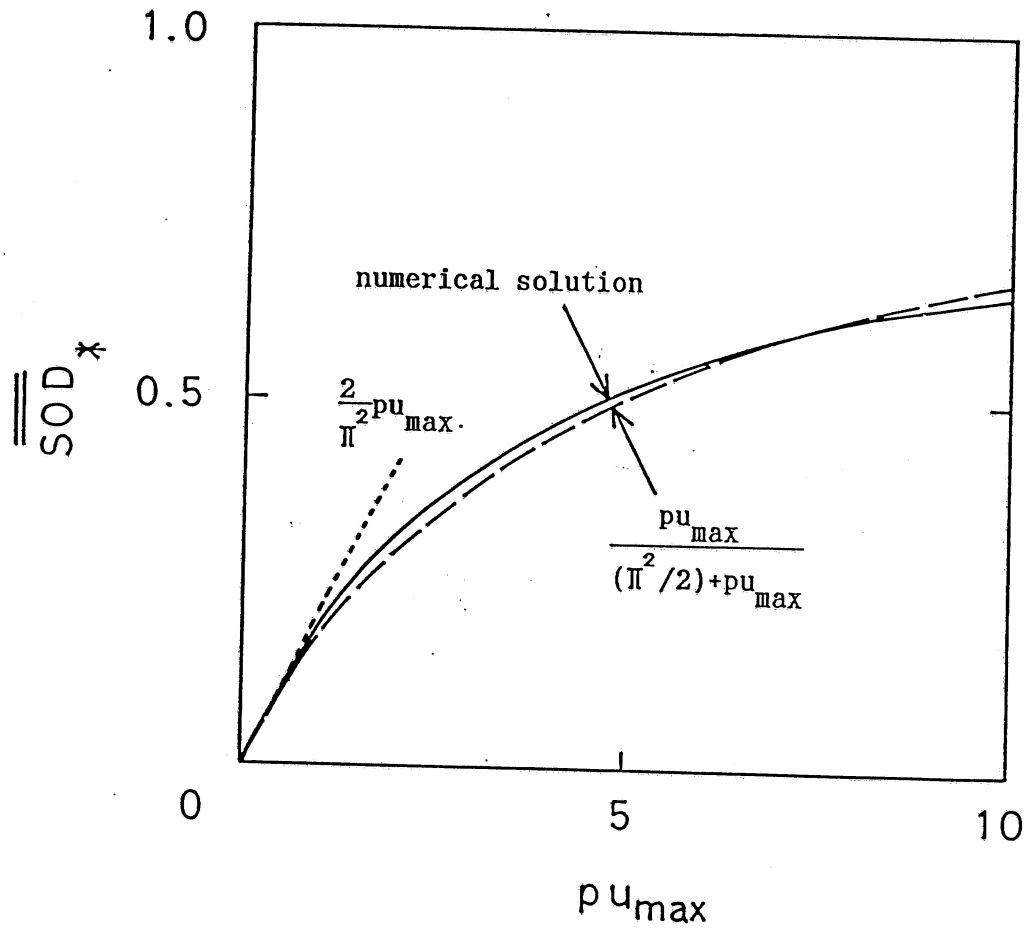

Fig. 15. Non–dimensional, space and time averaged SOD in a rectangular, two–layered lake as function of non–dimensional maximum velocity due to internal standing wave. Dotted line represents an asymptotic solution at low velocity. Broken curve denotes a proposed approximate function of averaged SOD.

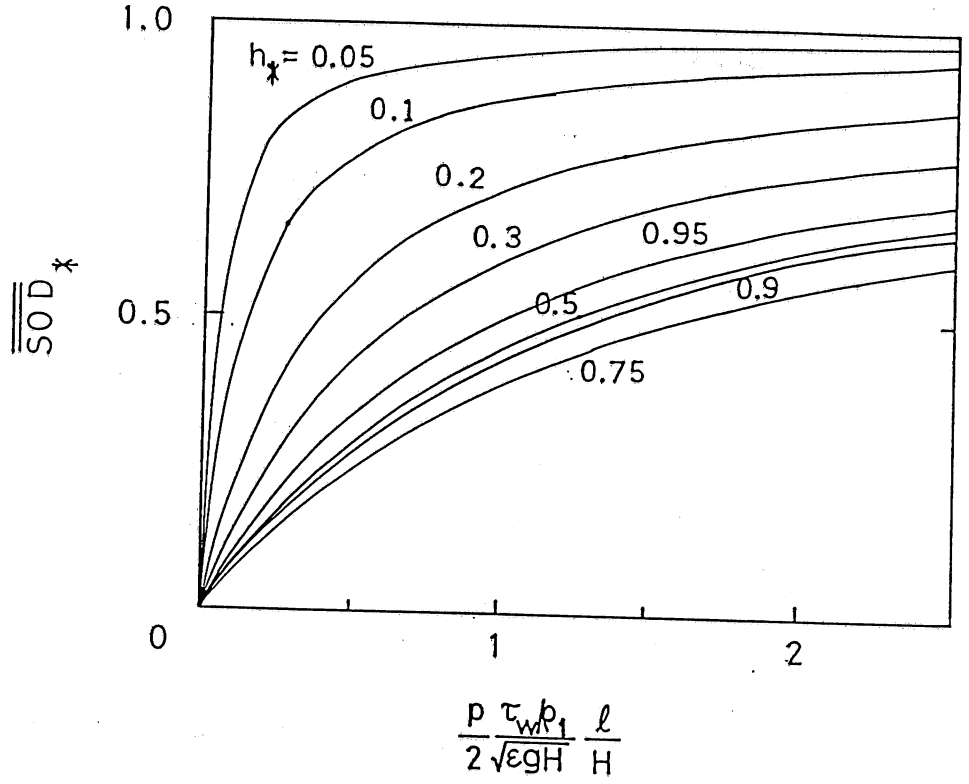

Fig. 16. SOD averaged over time and bottom area in a two–layered lake versus non–dimensional parameter including wind shear and fetch. h_* is the relative depth of the hypolimnion.

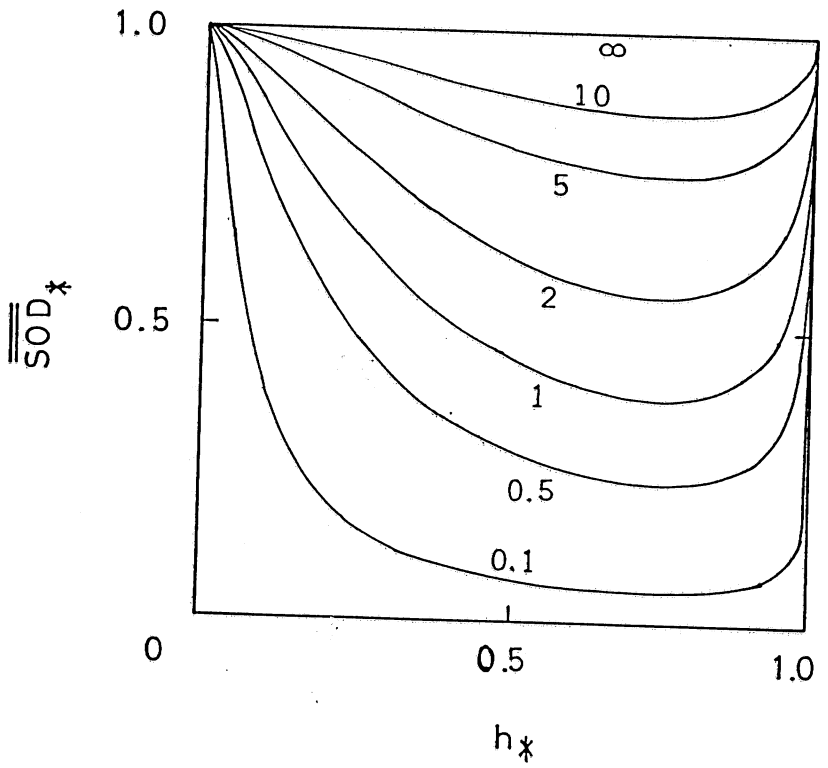

Fig. 17. SOD averaged over time and bottom area in a two–layered lake versus non–dimensional depth of the hypolimnion. τ_* is the windshear parameter.